SETTING OF THE ~2560 Ma QÔRQUT GRANITE COMPLEX IN THE ARCHEAN CRUSTAL EVOLUTION OF SOUTHERN WEST GREENLAND

ALLEN P. NUTMAN[*,**,***†] CLARK R.L. FRIEND[*], and JOE HIESS[***,****]

[*]Beijing SHRIMP Center, Chinese Academy of Geological Sciences,
26, Baiwanzhuang Road, Beijing, 100037, China
[**]School of Earth and Environmental Sciences, University of Wollongong,
Wollongong, NSW, 2522, Australia
[***]Research School of Earth Sciences, Australian National University, Canberra,
ACT, 0200, Australia
[****]NERC Isotope Geosciences Laboratory, British Geological Survey, Keyworth,
Nottinghamshire, NG12 5GG, U.K.

[†]Corresponding author: E-mail: allen.nutman@gmail.com

ABSTRACT. The Archean gneiss complex of West Greenland contains packages of unrelated rocks created during relatively short periods of time in arc-like magmatic environments, and having similarities to rocks formed at Phanerozoic convergent plate boundaries. The terranes of new Archean crust were amalgamated by collisional orogeny and then partitioned by post-assembly tectonic processes. Having summarised the origin of West Greenland Archean crust in arc-like environments, this paper then focuses on new data concerning the latest Neoarchean post terrane-assembly 'intra-continental' tectonic and magmatic evolution of the region.

Following the youngest documented high pressure metamorphism in a clockwise P-T-t loop at ~2650 Ma attributed to collisional thickening of the crust, there is in West Greenland a 150 million year record of intermittent production of crustally-derived granite, shearing and folding under amphibolite facies conditions. This is exemplified by the SSW-NNE orientated Neoarchean Qôrqut Granite Complex (QGC) which forms a myriad of closely spaced coeval sheets NE of Nuuk town. SHRIMP U-Pb zircon dating of a homogeneous grey granite sheet gives a magmatic age of 2561±11 Ma, with 3800-3600 and 3070-2970 Ma zircon xenocrysts. The >40 km long Færingehavn straight belt, a lower amphibolite-facies vertical shear zone, runs from the QGC's SE margin and contains strongly deformed granite sheets with a U-Pb zircon age of 2565±8 Ma but is cut by undeformed granite sheets dated at 2555±12 Ma. The >60 km long Ivisaartoq fault consisting of lowermost amphibolite-facies mylonite runs from the northwestern end of the main mass of granite. It formed post-2630 Ma, because granites of that age are truncated by it. Near the QGC's northeastern extent, 2559±3 Ma granitic lithons in a folded mylonite are cut by 2521±72 Ma granite sheets. At a deep structural level at the northern end of the QGC, deformed granitic neosomes give ages of 2567±9 and 2567±9 Ma. Therefore, at ~2560 Ma, the ages within error for strongly deformed to non-deformed granite bodies shows that the QGC is not a largely post-kinematic intrusion as previously thought, but was coeval with lowermost amphibolite-facies metamorphism and shear zones with important strike slip component, late in the development of regional non-cylindrical upright folds. The main body of the QGC appears to be essentially post-kinematic, only because it was emplaced in a node of dilation, during the heterogeneous predominantly strike slip deformation. Melting at this

node may have been triggered by meteoric water peculating down dilational fractures, causing metasomatism. Melting of these altered rocks gave rise to the low δ^{18}O signature of QGC igneous zircons. Due to the hydrous nature of the melting event, the QGC was emplaced immediately above its migmatitic generation zone. These late Neoarchean shear zones of the Nuuk region partition and disrupt the earlier-formed mosaic of amalgamated terranes of unrelated rocks. Such tectonic patterns are seen more recently, for example in Holocene Asian intra-continental tectonics along the north side of the Himalayas.

Keywords: Greenland; Neoarchean; Intra-continental tectonics; Qôrqut Granite Complex; shear zones; Zircon and monazite U-Pb dating

INTRODUCTION

Archean gneiss complexes are both geologically monotonous and bewilderingly complex. As seen in Greenland, they are monotonous because of their general lithological uniformity, being composed by volume >80% banded grey (ortho)gneisses, ≤10% amphibolites derived from volcanic rocks and gabbros, ≤10% granites and a few percent of metasedimentary rocks and mafic dikes. They are bewildering because on single outcrops they display complexity in their structures, with commonly evidence of many episodes of folding and metamorphism. Modern structural methodologies, particularly (a) the recognition of strain partitioning, (b) that 'D1' at separate localities may not be the same (see for example, Nutman and others, 1989), (c) the identification and mapping of early layer-parallel high-grade mylonite zones (see for example, Friend and others 1987, 1988), and (d) the greater integration of these field-based structural observations with U-Pb zircon geochronology (for example, Friend and others, 1996; Crowley, 2002; Nutman and Friend, 2007) provide further constraints on the origin and evolution of Archean gneiss complexes in southern West Greenland.

In the Nuuk region of southern West Greenland (fig. 1), the gneiss complexes are regarded as tectonostratigraphic terranes (*sensu* Coney and others, 1980) that consist mostly of meta-igneous rocks formed from several arc complexes (Friend and others, 1988; Nutman and others, 1989; McGregor and others, 1991). These were tectonically juxtaposed, sometimes with transient high-pressure metamorphism with clockwise P-T-t (pressure, temperature, time) loops (Nutman and others, 1989;

Nutman and Friend, 2007), followed by continued shearing under amphibolite facies metamorphism with emplacement of crustally-derived granites (McGregor and others, 1991). Thus Archean gneiss complexes contain a record of several important phases of modern-style tectonic activity – crustal accretion/formation in magmatic arcs, collisional orogeny and continued ‘intra-continental’ tectonics in laterally extensive bodies of assembled sialic crust. After outlining the Archean accretionary and collisional phases of tectonic activity in the Nuuk district, most attention in this paper will be paid to the intra-continental tectonics phase, particularly by discussing the origin and accommodation of the late Neoarchean Qôrqut Granite Complex (McGregor, 1973; Friend and others, 1985), which transgresses several terrane boundaries (fig. 1).

SUMMARY OF THE ARCHEAN GNEISS COMPLEX IN THE NUUK REGION

Recognition of juvenile tonalitic crust of vastly different ages and crustally-derived granites

In the Nuuk region, the first modern breakthrough in understanding Archean gneiss complexes was the realisation that the banded grey gneisses are largely derived from plutonic protoliths, particularly of tonalitic composition (McGregor, 1973), rather than being quartzo-feldspathic detrital metasedimentary rocks – a view widely adhered to up to the early 1970s (see discussion by McGregor, 1979). These orthogneiss complexes were recognised as the country rocks to late kinematic granite intrusions in the region (McGregor, 1973), particularly the *Qôrqut Granite Complex* (QGC), which is the main focus of this paper. The QGC is named after Qôrqut (the old Greenlandic orthography for Qooqqut) a fjord branch ~40 km east of Nuuk (fig. 1).

A contemporaneous second major breakthrough was the application of Pb-Pb and Rb-Sr whole rock geochronology to the Nuuk region gneisses and QGC. This revealed that the tonalite protoliths to the orthogneisses are of two generations, and each represents juvenile additions to the crust (Moorbath and others, 1972; Moorbath and Pankhurst, 1976). These were an Eoarchean suite (>3600 Ma), then known as the *Amîtsoq gneisses* cut by deformed amphibolitized diabase dikes (the *Ameralik dykes*) and a Meso- to Neoarchean suite (3100-2800 Ma), then known as the *Nûk gneisses*, not cut by amphibolitized diabase dikes (Black and others, 1971; McGregor, 1973). For the QGC, the first reliable dates were 2530±30 Ma recorded by bulk zircon U-Pb (Baadsgaard, 1976), a whole rock Rb-Sr isochron age of 2530±30 Ma and a Pb-Pb whole rock isochron age of 2580±80 Ma (Moorbath and others, 1981).

The integration of the 1970s fieldwork and isotopic dating led to the adoption of a broadly uniformitarian interpretation for the orthogneisses - that they were mostly calc-alkaline igneous suites formed at ancient convergent plate boundaries. This setting was certainly mentioned by 1972 (Moorbath and others, 1972). These complexes once formed were subject to protracted tectonothermal histories, with intrusion of crustally-derived granites such as the QGC.

Throughout the 1970s the accepted model for the Nuuk region Archean geology (McGregor, 1973) was its fundamental division into an Eoarchean gneiss complex (the Amîtsoq gneisses) – now known as the Itsaq Gneiss Complex (Nutman and others, 1996) tectonically intercalated with younger metavolcanic and metasedimentary units (the *Malene supracrustal rocks*), which were then both intruded by the Meso- Neoarchean Nûk gneisses, and then finally intruded by the essentially non-deformed QGC.

Recognition of tectonstratigraphic terranes

In the early 1980s, geological disagreements concerning the interpretation of some rocks from field versus isotopic perspectives (the Kangimut sammissoq controversy; Moorbath and others, 1986; Nutman and others, 1988) caused this model to be questioned, particularly the concept that any rocks cut by amphibolitized diabase dikes had to be Eoarchean. Due to this, Friend and Nutman remapped some of the contentious areas, particularly the edge of the granulite-facies area south of Nuuk in the Færingehavn area (fig. 2; Friend and others, 1987) and discovered that domains of gneisses with contrasting protolith age and metamorphic history were in folded Archean tectonic contact with each other. Combined with preliminary U-Pb zircon dating (Nutman and others, 1989), it was then proposed that the entire Nuuk region should be divided into Archean terranes bounded by mylonites that are subsequently folded and metamorphosed under amphibolite-facies conditions. This allowed previous detailed structural studies from small parts of the Nuuk region (for example, Berthelsen, 1960; Bridgwater and others, 1974; Chadwick and Nutman, 1979) to be placed into a new large-scale context. Each of the terranes consists of broadly similar-looking but different-aged Archean orthogneisses largely derived from tonalites and granodiorites, which evolved separately prior to later Archean tectonic juxtaposition and a common later Archean history (Friend and others, 1988; Nutman and others, 1989). The fundamental difference between this and the McGregor (1973) interpretation is that different units of orthogneisses can be in tectonic contact with each other, whereas in the McGregor model the igneous protoliths of all groups of orthogneisses initially had intrusive relationships. This new terrane interpretation was adopted by McGregor and others (1991) in a new Archean plate tectonic synthesis for the Nuuk region (for example, fig. 3 of that paper), which by then was divided into four tectonostratigraphic terranes. This reinterpretation saw each terrane as largely juvenile crustal components formed in ancient analogues of magmatic arcs at modern-style plate boundaries (for example, Nutman and others, 1989). This model is entirely in accord with plate tectonic processes in the broadest sense, with the recognition of arc-like chemical signatures in both felsic and mafic rocks (for example, Steenfelt and others, 2005; Garde, 2007; Polat and others, 2008) and clockwise P-T-t metamorphic events related to tectonic crustal thickening during collisional orogeny between some terranes (Nutman and others, 1989; Nutman and Friend, 2007). This model continues to develop as geological mapping continues and further zircon U-Pb geochronology becomes available (fig. 3). The details of the terrane model across this vast, geologically-complex, region are continually being revised, particularly with the recognition of new terranes and better demarcation of their boundaries (for example, Friend and Nutman, 2005). The model has endured scrutiny by Crowley (2002) who from his detailed integrated structural and U-Pb mineral dating study agreed with our previous findings. A modified version of the terrane model (Windley and Garde, 2009; Keulen and others, 2009) is explored in the Discussion section of this paper.

Polymetamorphism and prograde and retrograde amphibolite – granulite-facies transitions

Wells (1976) made an important contribution to understanding the Nuuk region orthogneisses and similar rocks the world over by demonstrating using cation exchange thermobarometry that granulite-facies rocks south of Nuuk (a ~2800 Ma metamorphic event in the Tasiusarsuaq terrane – for example Crowley, 2002) experienced conditions of ~800°C and 8-9 Kbar. The moderately high pressures demonstrated perhaps for the first time that Archean continental crust could be of considerable thickness, and was not thin and mobile as was commonly thought before the early 1970s. However, few gneiss outcrops in the Nuuk region show evidence of only one episode of high-grade metamorphism. This indicates the complexity in the region’s crustal evolution. Thus granulite-facies rocks commonly show evidence of retrogression under amphibolite-facies conditions, which when coupled with strong later ductile deformation can obliterate the evidence for former granulite-facies conditions (for example, Friend and others, 1987). Also mineral corona structures and compositional zoning point to the complexity of the metamorphic history (for example Griffin and others, 1980; Rollinson, 2003).

With the commissioning of the SHRIMP-I ion microprobe in the early 1980s, it became possible to produce accurate and precise ages of metamorphism in the Nuuk region by U-Pb dating of generally low Th/U zircon rims interpreted to have formed during metamorphism (fig. 3). Early SHRIMP studies indicated a range of ages for Neoarchean metamorphism from ~2820 to ~2650 Ma, well beyond analytical error (Kinny, 1986; Schiøtte and others, 1988, 1989), confirming the indication of metamorphic complexity based on field and petrographic observations. This range of metamorphic ages has been placed into a detailed tectonic framework, relating to the production of arc crust within each terrane, followed by metamorphism during and after collision of terranes (fig. 3; for example see Garde and others, 2000; Crowley, 2002; Friend and Nutman, 2005; Nutman and others, 2007 for dating of different metamorphic events). Amphibolite-facies metamorphism continued until intrusion of the QGC at ~2560 Ma (fig. 3). The dating and significance of this metamorphism is investigated below.

Relicts of high-pressure metamorphism

Terrane juxtaposition was followed by Neoarchean folding under amphibolite facies conditions, with widespread low-pressure recrystallisation (5-4 kbar and 700-550°C; Nutman and others, 1989; Nutman and Friend, 2007). The complex metamorphic overprinting requires determining the P-T history from relicts of older metamorphic assemblages. P-T-t studies are complimented by petrographic studies and examining the geochemistry of metamorphic zircons.

In the south of the Nuuk region, the Færingehavn terrane (Eoarchean in age and dominated by orthogneisses) is tectonically overlain by an unnamed slice of amphibolites and paragneisses (~2840 Ma felsic volcano-sedimentary protoliths). This is juxtaposed against a higher tectonic level represented by the Tre Brødre terrane (2825 Ma orthogneisses *without* ~2800 Ma granulite facies metamorphism) and the Tasiusarsuaq terrane (dominated by 2920-2810 Ma orthogneisses *with* ~2800 Ma granulite facies metamorphism). The terranes were assembled by 2710-2720 Ma (fig. 3), as shown by dating of granitic sheets intruded along the terrane boundary mylonites (Crowley, 2002; Nutman and Friend, 2007). In the Færingehavn terrane and in the overlying 2840 Ma supracrustal slice, relict high-pressure assemblages (12-8 kbar, 750-700°C) are clinopyroxene + garnet + plagioclase + quartz ± hornblende in mafic rocks and garnet + kyanite + rutile bearing assemblages in paragneisses. These are mostly replaced by lower pressure (7-5 kbar) assemblages of cordierite ± sillimanite ± garnet in paragneisses and hornblende + plagioclase + quartz ± garnet *or* clinopyroxene in amphibolites. *In situ* partial melting took place during low- *and* high-pressure regimes (Nutman and Friend, 2007). Metamorphic zircon in the high- and low-pressure assemblages yields dates of ~2715 Ma, mostly with errors of < ±5 Ma, thereby demonstrating rapid high temperature decompression. Zircons in the overlying Tre Brødre and Tasiusarsuaq terranes show little response to the ~2715 Ma event supporting structural interpretations that they were at a higher crustal level at this time (Nutman and Friend, 2007).

The Kapisilik terrane consisting of largely 3050-2960 Ma orthogneisses and supracrustal rocks (Friend and Nutman, 2005) and a supracrustal assemblage of ~2800 Ma amphibolites and quartzo-feldspathic metasedimentary rocks, occurs north of the Færingehavn terrane and is bounded by folded Neoarchean mylonites (fig. 4). Where the ~2800 Ma supracrustal assemblage occurs near the southern edge of the Kapisilik terrane, it has rare high-pressure metamorphic remnants in amphibolites and metasediments (metamorphic segregations with garnet + clinopyroxene and kyanite respectively) that formed at ~2650 Ma. Thus remnants of early metamorphism reveal mutually exclusive ~2715 and ~2650 M high-pressure events in adjacent tectonically juxtaposed terranes (figs. 3 and 4).

Metamorphic petrology, zircon dating and zircon trace element chemistry and zircon inclusion suites are consistent with metamorphic events along clockwise P-T-t loops (Nutman and Friend, 2007). Such P-T-t trajectories with relict high-pressure granulite-facies assemblages are the hallmark of tectonic thickening of the crust during collisional orogeny (O'Brien and Rötzler, 2003; Pattison, 2003).

Post-2650 Ma Archean 'intra-continental' events in the Nuuk region

A ~2650 Ma clockwise P-T-t loop recorded in Neoarchean supracrustal rocks along the southern edge of the Mesoarchean Kapisilik terrane in the northeastern part of Godthåbsfjord (fig. 4) is inferred to be the youngest Archean collisional orogenic event in the Nuuk region. Subsequent events in the remainder of the Neoarchean were of 'intra-continental' character, involving partitioning and disruption of the earlier assembled terranes (Nutman and Friend, 2007). This is expressed by repeated shearing, folding and granite intrusion, mainly under low amphibolite-facies conditions at moderate pressures (Dymek, 1983; Nutman and others, 1989). There is widespread evidence of several events from the U-Pb dating of (a) metamorphic overgrowths and recrystallisation of zircons in gneisses, (b) igneous zircons in granites and pegmatites and (c) titanites and monazites, that give widespread evidence of a complex tectonothermal history after 2650 Ma, with separate events now recognised at ca. 2630, 2610, 2580, 2560 and 2540 Ma (fig. 3; for example Schiøtte and others, 1989; Crowley, 2002; Nutman and others, 2004; Nutman and Friend, 2007). Important gold mineralization is associated with this activity, such as at ~2630 Ma on the island of Storø (Nutman and others, 2007). This activity is too extensive to be covered here in its entirety. Instead we focus on the age, structural setting and origin of the QGC, which is the largest and best-known of the late Neoarchean granites in the Nuuk region.

QÔRQUT GRANITE COMPLEX (QGC)

Field geology and structure

Granites and granite pegmatites comprising the ~2560 Ma QGC occur in a SSW-NNE trending linear belt >150 km long extending through the Buksefjorden-Ameralik- Godthåbsfjord part of the Nuuk region (fig. 1; McGregor, 1973; Brown and others, 1981; Friend and others, 1985). Additionally, granite sheets as far northeast as Ivisaartoq have been correlated with the QGC on the basis of their lack of deformation compared with their host gneisses (Friend and Hall, 1977). The main body of the complex crops out over a distance of ~50 km from Ameralik to Kapisillit kangerdluat and reaches a maximum outcrop width of 18 km between Storø and Qooqqut. All known components of the QGC are essentially true granites in composition and primarily carry biotite rather than muscovite or garnet. No coeval mafic rocks have yet been found associated with it.

Detailed 1:20,000 scale mapping of the main part of the granite showed that it is not a single massive intrusion, but consists of myriads of inclined granite sheets, emplaced at the same crustal level (fig. 5A; Brown and others, 1981; Friend and others, 1985). In the main part of the QGC, the granite sheets were inferred to be emplaced passively along brittle to semi-brittle dilational fractures (Friend and others, 1985). Around Qooqqut the QGC comprises three main groups of granites: early leucocratic granites, various grey biotite granites, and late aplogranite granite pegmatites. In one 1500 m vertical section mapped in the central part of the complex, the complex has a tripartite structure comprising a lower zone dominantly of polyphase granite, an intermediate zone where country rock occurs as rafts in polyphase granite with a complex sheeted structure, and an upper zone dominantly of country rock sheeted by granite. Most of the granite sheets in this part of the complex dip gently westwards (Friend and others, 1985). In peripheral areas to the southwest and northeast, there are local concentrations of pegmatite and granite that have locally coalesced into continuous outcrops of granite (fig. 5B). Prominent occurrences of these are on the southern side of the Narssaq peninsular and at Skindehvalen, northwest of Færingehavn (fig. 1). Some of these granite sheets are shallowly inclined, whereas others strike ESE and are dip close to vertical or steeply north.

The overall form of the QGC plunges gently SSW more or less coaxial with late upright folds of that orientation. Therefore the granite and pegmatite sheets on the low lying islands and coastline to the SSW might correlate with the upper parts of the complex exposed at >1000 m altitude around Qooqqut (fig. 1). Furthermore, north of Kapisillit kangerdluat, granite sheets are rare at sea level, but instead there is a concentration of them at an altitude of >1000 m. On the other hand, at the northern end of the QGC, our geochronology has revealed that migmatites with ~2560 Ma QGC-aged components are common at sea level.

Locally, Brown and others (1981) and Friend and others (1985) noted the QGC to be cut by shear zones, and that the main body of granite was emplaced into an antiformal structure with essentially the same trend as regional late upright folds in the country rocks. Moreover, locally sheets of non-deformed granite cut granite sheets that appear to be deformed. They also noted that the QGC appeared to truncate a major vertical amphibolite facies shear zone at its southern end – a structure discussed here as the Færingehavn straight belt (figs. 1 and 2). They also remarked on the presence of a similar shear zone to the west of the main occurrence of the granite, in which sheets of granites considered to be of QGC age are found variably deformed.

On the north side of Ameralik, at the southern contact of the complex (that dips steeply to the SSW), peculiar feature is the strong bleaching of the marginal country rocks to the granite. For >1 km towards this upper margin of the granite, the heterogeneity of the banded country migmatitic gneisses is progressively erased, and the rocks assume a homogeneous bleached buff-white to pink tone. The boundary between these modified country rocks and the main granite body is sharp and clearly intrusive, and not gradational. Therefore there is no sign of *in situ* partial melting associated with this change at the upper contact. In the absence of *in situ* melting, these changes are attributed to hydrous metasomatism (see below). This contrasts with features farther to the north (as around the entrance to Kapisillit kangerdluat) structurally near the base of the granite, where there is clear evidence of *in situ* melting of the country rocks.

Previous interpretations, geochemical and isotopic constraints

Whole-rock geochemical analyses of the granite coincide with the experimental eutectic in the granite system at ~5 kbar, suggesting minimum melting of country quartzofeldspathic orthogneisses and emplacement at mid-crustal levels (Brown and others, 1981). This is in accord with migmatisation of country gneisses at deep structural levels of the granite (Brown and others, 1981; Friend and others, 1985; this paper). From their geochemical modeling, Brown and others (1981) remarked that melting required not only a heat source, but fluid as well. They suggested that both were derived from depth or that the fluid was obtained solely by breakdown of hydrous phases in the country rocks. In this paper we provide evidence that influx of meteoric water into the mid-levels of the crust might have occurred.

Moorbath and others (1981) presented Pb-isotopic results on QGC samples. They concluded that the granite was produced by intracrustal melting of a mixture of Mesoarchean gneisses, like those cropping out immediately to the west of the QGC, plus Eoarchean rocks. Evidence of contribution of juvenile ~2560 Ma material to the formation of the granite is lacking. The mixed Meso- Eoarchean crustal source for the granite corroborated here by the dating of zircon xenocrysts from the granite.

Generally, the QGC has been regarded as an essentially post-kinematic intrusion, at the termination of Archean granite emplacement in the Nuuk region. Presented here are structural studies integrated with U-Pb zircon geochronology, which have resulted in a revised interpretation. Instead we see the granite as an integral part of long-lived intermittent focused deformation and high heat flow, with resultant anatexis, shear zone formation and folding under amphibolite facies conditions. Geochronological data presented here indicates that this activity outlasted the emplacement of the QGC by >30 million years.

SHRIMP U-PB ZIRCON AND MONAZITE GEOCHRONOLOGY

U-Pb zircon and monazite dating in this contribution were mostly undertaken on the SHRIMP-I instrument in the Australian National University (ANU), with a lesser amount undertaken on the ANU SHRIMP-II and –RG instruments. Analytical methods follow those given by Williams (1998) and Stern (1998), but see the Appendix for further background information on methods. The main focus is on zircon geochronology, because monazite is a rare phase in the Nuuk region gneisses.

Main body of the QGC and satellite pegmatite and granite sheet swarms

Sample 195376 of a homogeneous grey granite sheet from the north-central part of the QGC (fig, 1; at Google Earth™ 64º24.16'N 50º54.94'W) yielded structurally complex zircons. SHRIMP U-Pb zircon analyses were undertaken in the early 1990s, without the benefit of CL imaging. None the less, composite structure of the zircons is visible by transmitted and reflected light microscopy (denoted by 'c' in the second column of table 1). Analyses of structural cores yielded two groups of U-Pb ages. Those with $^{207}Pb/^{206}Pb$ ages >3400 Ma form a discordant array intersecting concordia between 3800-3600 Ma (fig. 6A). Three analyses of the core of grain 14 scatter across concordia, with an intercept at 3717±88 Ma. Two of these analyses are distinctly reverse discordant, with apparent $^{207}Pb/^{206}Pb$ ages up to 3933±42 Ma (2σ) (table 1, fig. 6A). This core is thus interpreted to have an age of ~3720 Ma, and to contain domains where radiogenic Pb is in deficit or excess relative to local U content, due to Pb-movement in an ancient event. Excess of radiogenic Pb in zircons is rare, but has been documented from other high-grade gneiss terranes (for example, Williams and others, 1984). The second group of inherited cores are Mesoarchean in age, and all have close to concordant U-Pb ages, with $^{207}Pb/^{206}Pb$ ages between ~3070 and 2980 Ma, matching the age of rocks in both the Akia and Kapisilik terranes (for example Garde and others, 2000; Friend and Nutman, 2005). Mantles of these cores and structureless oscillatory zoned prisms have generally higher U abundance than the cores and close to concordant Neoarchean U-Pb ages, with a weighted mean $^{207}Pb/^{206}Pb$ age of 2561±11 Ma (table 1; figs. 6A and B). 2561±11 Ma interpreted as the age of crystallisation and emplacement of this grey granite component of the QGC.

A few analyses of zircons from a ~10 m thick granite sheet on the south coast of Kapisillit fjord (fig, 4; G87/218, at Google Earth™ 64°24.2'N 50°31.0'W) and a mass of sheeted granite on the hill Skindehvalen north of Færingehavn (fig. 2; G84/12 at Google Earth™ 63°44.3'N 51°33.0'W) are reported here (table 1). These were part of a reconnaissance dating study undertaken in 1990 by H. Baadsgaard and A. Nutman, to assess the extent and age-range of late Neoarchean magmatism in the region. Two analyses on G87/218 igneous oscillatory-zoned prismatic grains gave close to concordant U-Pb data (table 1), with a weighted mean $^{207}Pb/^{206}Pb$ age of 2559±5 Ma, indistinguishable from the age of the main body of QGC to the west. Two analyses were undertaken on G84/12 zircons, both of which gave U-Pb ages concordant within analytical error (table 1). An analysis of an oscillatory-zoned prismatic zircon yielded a $^{207}Pb/^{206}Pb$ age of 2552±8 Ma (2σ), whereas an analysis of a structural core gave a $^{207}Pb/^{206}Pb$ age of 2732±12 Ma (2σ). The former is interpreted as an igneous grain, showing that the granite at Skindehvalen probably has a similar age to the main body of the QGC. The core analysis has an age matching a period of earlier migmatisation and granite emplacement in the southern part of the Nuuk region (Friend and others, 1988; Crowley, 2002; Nutman and Friend, 2007).

Færingehavn straight belt and Ivisaartoq fault

The Færingehavn straight belt, first identified in 1:20,000 scale regional mapping at Færingehavn by Sharpe (1975) and studied further north by Gibbs (1976) is a 1-2 km wide ductile shear zone (fig. 1), in which the rocks have a ~NNE-striking steep foliation and shallow SSW-plunging mineral lineations. Metamorphic assemblages in the belt at Færingehavn reflect low amphibolite-facies metamorphism assessed at 550-500°C and 5-4 kbar by cation exchange thermobarometry (Nutman and others, 1989). South of Færingehavn, the straight belt passes out to sea, and to the north it continues to Ameralik, were it meets the southeastern corner of the main body of the QGC (fig. 1; Friend and others, 1985). It is clearly a late structure, because granite sheets belonging to the ~2550 Ma body of granite forming Skindehvalen (fig. 2) are deformed within it. This has been tested by dating variably deformed granite sheets on the islet Smukke Ø in fjord entrance south of Færingehavn (figs. 1 and 2, at Google Earth™ 63°41.06'N 51°32.37'W). On this islet, strongly deformed Eoarchaean orthogneisses of the Itsaq Gneiss Complex have numerous subconcordant sheets and lenses of granite (sample G85/382), which in turn are cut by less deformed, discordant granite sheets (sample G85/383). Ages from IDTIMS U-Pb bulk zircon fractions from samples G85/382 and G85/383 yielded slightly discordant data with $^{207}Pb/^{206}Pb$ ages of ~2500 Ma, indicating latest Archean movement (Nutman and others, 1989). SHRIMP U-Pb dating of zircons from both these samples are presented here. Both contain oscillatory-zoned prismatic zircon (figs 7A and B), with no inherited components detected. U-Pb ages from both samples are mostly concordant within error (table 1; figs. 8A and B), with the strongly deformed granite sheets concordant with the Færingehavn straight belt fabric yielding a weighted mean $^{207}Pb/^{206}Pb$ age of 2565±8 Ma, whereas those from the discordant less deformed sheet G85/383 yield an indistinguishable $^{207}Pb/^{206}Pb$ weighted mean age of 2555±12 Ma. This shows that movement on the Færingehavn straight belt was coeval with the intrusion of the QGC.

At the northwestern corner of the main body of the QGC, we propose there is another NNE-striking steep low amphibolite-facies shear zone, complementing the Færingehavn straight belt in the south (fig. 1). This structure is neither as well exposed, nor are there so rigorous U-Pb zircon age constraints on the timing of its movement. It has been named the Ivisaartoq fault (Nutman and Friend, 2007), after the locality at its northern end where it is best exposed. On Ivisaartoq it cuts through the western limb of the ~3070 Ma (Friend and Nutman, 2005) Ivisaartoq supracrustal belt, within the Kapisilik terrane (fig. 1). On the east side of the straight belt, granite sheets with an age of ~2630 Ma (Nutman and Friend, 2007) are truncated at the margin of the fault, in which they are transformed into mylonite. Therefore the Ivisaartoq fault formed post-2630 Ma, and hence could be coeval with the syn-QGC Færingehavn straight belt in the south. Along its projected strike to the south on the island of Uummannaq (west of the mouth of the fjord leading to Kapisillit – fig. 1), the fault occurs between Itsaq gneiss complex orthogneisses dated at ~3730 Ma (Bennett and others, 1993), and different undated homogeneous orthogneisses to the west.

There have been no systematic studies on the kinematic evolution of the Færingehavn straight belt and the Ivisaartoq fault. Where the Ivisaartoq fault cuts through the Ivisaartoq supracrustal belt, disrupted (~2630 Ma) granite sheets in amphibolite schists form sigmoidal lenses with a symmetry indicating some sinistral movement on the fault.

Migmatites and folded mylonites at the northern end of the QGC

Weakly deformed neosome 480115. At sea level north of the entrance to Kapisillit fjord, migmatitic gneisses are commonly overprinted by domains of *in situ* neosome development with biotite as the main ferromagnesian phase, plus sheets of fine-grained biotite granite. The neosome is interpreted as arrested wet-partial melting, and the sheets are interpreted as coalesced bodies formed out of that process. The neosome and granite sheets are weakly deformed, with the latter showing podding, with the boudin necks occupied by locally-formed pegmatite. The style of deformation suggests syn-magmatic extension (fig. 9A). Sample 480115 (fig. 4, at Google Earth™ 64°29.71'N 50°37.16'W) is *in situ* biotite-bearing neosome, tainted by small paleosome remnants. Most zircons from neosome 480115 are 100-200 µm long prisms with oscillatory zoning parallel to their margins. A few possible xenocrystic cores were detected in the CL images. The oscillatory zoning is rather dull and low contrast because of the generally high U content of the zircons, and is locally disrupted by recrystallisation domains. Analyses were undertaken on 21 grains. Xenocrystic cores gave ages >2600 Ma, with the oldest (analysis 15.1) being ≥3560 Ma (table 1). The main group of oscillatory zoned zircons can be divided into two groups (table 1, fig. 10A). A lesser number of analyses yield ages of ca. 2590 Ma, which has previously been observed as a time of metamorphism and pegmatite injection in the Nuuk region (Nutman and Friend, 2007). The majority of igneous zircons gave close to concordant U-Pb ages, with a weighted mean $^{207}Pb/^{206}Pb$ age of 2567±9 Ma. Thus this migmatite has a complex history, but the zircon results suggest that the main phase of melting displayed by weakly deformed neosome probably occurred at 2567±9 Ma

Weakly deformed neosome 481415. QGC migmatite component, sample 481415 is from sea level on the southern side of the entrance to Kapisillit fjord (Google Earth™ 64°25.09'N 50°36.79'W), structurally below the large mass of QGC forming the ridge to the south (fig. 4). The country rocks here are polyphase Itsaq Gneiss Complex banded gneisses, which reconnaissance SHRIMP U-Pb zircon dating show to have an age of >3650 Ma (sample 437603 in Horie and others in press). These Itsaq Gneiss Complex rocks show widely developed *in situ* partial melt neosomes, which merge into coalescing cross-cutting granite sheets. Both the neosome and the granite sheets are locally weakly deformed (fig. 9B). Biotite is the main ferromagnesian mineral in the neosomes, indicating wet melting. The zircons typically have well formed prismatic habits and oscillatory growth zonation while some domains are recrystallized or homogeneous in CL. The zircons can be divided into three age populations. The oldest Eoarchean population consists of 8 analyses, with $^{207}Pb/^{206}Pb$ ages ranging from 3659±5 Ma to 3338±7 Ma, with a weighted mean of

3652±12 Ma for 4 spots >3610 Ma (table 1). U concentrations ranged from 110 to 1565 ppm and Th/U ratios ranged from 0.02 to 0.86. A ~2700 Ma Neoarchean population consists of 7 U-Pb analyses, with $^{207}Pb/^{206}Pb$ ages ranging from 2818±18 Ma to 2646±18 Ma, and a weighted mean age of 2700±9 Ma for 5 spots (fig. 10B). U concentrations ranged from 159 to 2778 ppm and Th/U ratios ranged from 0.07 to 1.00. The youngest ~2560 Ma Neoarchean population consists of 14 U-Pb analyses, with $^{207}Pb/^{206}Pb$ ages ranging from 2615±3 Ma to 2472±5 Ma, with a weighted mean of 2563±5 Ma for 11 spots >2500 Ma and <2600 Ma (fig. 10B). Th/U ratios ranged from 0.03 to 0.8 while U concentrations were highly variable ranging from 108 to 7720 ppm. The U content of some grains was so high that their matrix contrasts with the significantly lower U concentration of the $^{206}Pb/^{238}U$ calibration standard. Subsequently these analyses appear as reversely discordant on the concordia diagram (fig. 10B) however $^{207}Pb/^{206}Pb$ ratios and ages are not affected by this problem. These results indicate that the Itsaq Gneiss Complex at this locality underwent high grade metamorphism with zircon growth at ca. 2700 Ma, upon which was superimposed *in situ* melting at 2563±5 Ma, coeval with the age of the QGC (exemplified by sample 195376).

Deformed migmatite 195392. At this coastal locality, the QGC granite sheets contain rafts of banded migmatite gneisses, which locally appear to merge into QGC granite which dominates cliffs above. Sample 195392 (fig. 1, at Google Earth™ 64°16.27’N 51°03.54’W) of the migmatite was chosen for zircon geochronology. This sample has a bulk granodioritic rather than granitic composition (Table 5 of Friend and others, 1985). It yielded a diverse population of variably rounded to prismatic zircons, which in CL images show complex core, rim/mantle and replacement textures (fig. 7c).

Structural cores of corroded and broken oscillatory zoned zircon have U-Pb ages from ~3700 to 2900 Ma, with the oldest yielding U-Pb ages concordant within error and the younger scattering around a ~3640 Ma to late Neoarchean discordia (fig. 10C; Hiess, 2008). For the oldest sites U concentrations were variable, ranging from

1476 to 42 ppm and Th/U ratios were also variable, ranging from 0.04 to 1.62. For the younger domains forming this discordant array, 6 analyses on grain cores provided $^{207}Pb/^{206}Pb$ ages ranging from ~3215 to 2980 Ma, with U concentrations ranging from 1291 to 43 ppm and Th/U from 0.75 to 0.08. A population of early Neoarchaean zircons with close to concordant U-Pb ages is also present (fig. 10C), upon which seven analyses were made, 2 on grain cores, 3 on grain mantles and 2 on grain edges. U concentrations ranged from 205 to 824 ppm and Th/U from 0.13 to 0.07. Rejecting one site that is interpreted to have lost some radiogenic Pb, the remaining 6 sites yielded a weighted mean $^{207}Pb/^{206}Pb$ age of 2726±5 Ma. Eight analyses yielded younger Neoarchean $^{207}Pb/^{206}Pb$ ages from 2572±17 Ma to 2541±16 Ma. U concentrations ranged from 42 to 1258 ppm and Th/U from 1.03 to 0.04. Two sites yielded exactly 2572 Ma, the age of a known marginally pre-QGC thermal event in the region (Nutman and Friend, 2007). With these two rejected, the remaining 6 analyses have a weighted mean age 2559±11 Ma. However if a more conservative approach is taken and the two 2572 Ma sites are included in the calculation, a weighted mean age 2570±4 Ma is obtained. Thus the sample is interpreted as an Eoarchean gneiss that underwent migmatization including anatexis and/or granite veining at both 2726±5 Ma, and then again at 2559±11 Ma. The latter event is within error of U-Pb ages obtained on QGC granites *sensu stricto*, such as 195376 with an age of 2561±11 Ma. (Fig. 10C; see also Hiess, 2008). This suggests that radiogenic Pb was lost from the cores mostly in the QGC event rather than the 2726 Ma migmatization.

Granitoid samples in meta-mylonite, 459808 and 459809. On the southern shoreline of Kapisillit fjord, folded metamylonite crops out west of Itinera (459808 locality on fig. 4, at Google Earth™ 64°23.43'N 50°42.70'W). The adjacent rocks to this mylonite are polyphase Itsaq Gneiss Complex banded gneisses, which reconnaissance SHRIMP U-Pb zircon dating show to have an age of ~3700 Ma (sample 437602 in Horie and others, in press). The biotite-rich mylonite groundmass is folded and contains lithons of granite and pegmatite, represented by granite sample 459809. These are clearly more deformed and disrupted than granitic sheets at the sample locality, which are concordant to the biotite foliation and have been folded (figs. 11A and B). These sheets are represented by sample 459808.

Zircons from granitic lithon 459809 encased within the mylonitic fabric are prismatic and 100 to 200 µm in length. Most grains are dark and structureless in CL but locally have faint oscillatory zonation. Seventeen U-Pb analyses, yielded $^{207}Pb/^{206}Pb$ ages ranging from 2568±4 Ma to 2499±20 Ma with two outliers at 2624±42 Ma and 2756±26 Ma (table 1, fig. 10D). The coherent population (n=15) record varying degrees of concordance and a weighted mean age of 2559±3 Ma. U concentrations are typically high, ranging from 605 to 4744 ppm and the Th/U ratios range from 1.58 to 0.05.

Zircons from granitic sheet 459808 are prismatic and 100 to 250 µm in length. Grains are generally dark and structureless in CL with a few inherited cores preserving clearly defined oscillatory zonation. 8 U-Pb analyses, record $^{207}Pb/^{206}Pb$ ages ranging from 2479±36 Ma to 2207±58 Ma with one outlier of an oscillatory zoned core at 3414±44 Ma (table 1). Within the young, discordant population U concentrations are high ranging from 1741 to 7586 ppm with high Th/U ratios, ranged from 6.56 to 1.70. Due to the micro-scale variation in U-Th-Pb count rates during the analysis of these disturbed zircons, they display large analytical errors – far beyond that expected from counting statistics alone. Furthermore the analyses of the young population (n=7) are highly discordant and form an array with intercepts at 2446±88 Ma and 25±31 Ma. Hence these data are presented in table 1 but they are not plotted on a Concordia diagram. 2446±88 Ma is an imprecise age for the intrusion of this granite sheet, and thereby a minimum age of much of the deformation in the mylonite.

Deformed granite sheet G01/107 in Ivinnguit fault amphibolite-facies mylonite, near Nuuk. Within the belt of supracrustal rocks forming the ridge Store Malene east of Nuuk, there is an amphibolite facies mylonite. This mylonite has been traced for >100 km and is known as the Ivinnguit fault (fig. 1; Friend and others, 1988). Along the Ivinnguit fault, amphibolites west of the mylonites are intruded by orthogneisses with igneous emplacement ages of ~3000 Ma, whereas to the east, paragneisses with 2900 Ma detrital zircons (Hollis and others 2005) are intruded by

~2825 Ma Ikkattoq gneisses (Nutman and Friend, 2007). Along Store Malene, the Ivinnguit fault, the ~2800 Ma rocks to the east and the ~3000 Ma rocks to the west are cut by anastomosing granite and pegmatite sheets. These sheets are variably deformed in the mylonites, where they can be found to cut strong mylonite fabrics, yet they themselves have developed a weaker fabric coplanar to the mylonites. Therefore the dating of such sheets will give the timing of late movement on the Ivinnguit fault.

Sample G01/107 is of a foliated granite sheet cutting mylonite, at Google Earth™ 64°10.33'N 51°35.67'W on Store Malene that yielded stubby brown-coloured zircons and yellow euhedral monazite crystals. In CL images the zircons are variably metamict, and care was needed to select domains showing the least recrystallization, with vestiges of igneous oscillatory zoning (fig. 7D). Some of the analyses are discordant, (fig. 12A) but most yielded close to concordant U-Pb data with a weighted mean $^{207}Pb/^{206}Pb$ age of 2531±4 Ma. Monazites appear to be structureless (fig. 7D) and most analyses of them yielded ages that are concordant within error and all have $^{207}Pb/^{206}Pb$ ages indistinguishable from each other (table 1, fig. 12B). Uncorrected for common Pb, they yielded a weighted mean $^{207}Pb/^{206}Pb$ age of 2536±5 Ma, and (over)corrected for common Pb they yielded an indistinguishable $^{207}Pb/^{206}Pb$ age of 2530±5 Ma. Thus the monazite age agrees with the age of igneous zircons at 2531±4 Ma, and shearing under amphibolite-facies conditions continued for at least 30 million years after the emplacement of the ~2560 Ma QGC.

Regional thermal environment of the QGC

Throughout the Nuuk region, metamorphic zircons with ages similar to the QGC have been detected intermittently in SHRIMP U-Pb mineral dating projects (for example, sample G88/77 in Nutman and Friend, 2007). Also, titanite and apatite U-Pb ages are commonly 2600 to 2500 Ma (Baadsgaard and others, 1976; Crowley, 2002). This is consistent with the margins of the QGC being devoid of a contact metamorphic aureole, and with the evidence that it was emplaced in the middle crust not far above its source region at an estimated 5 kbar (Brown and others, 1981; Friend and others, 1985). Furthermore, from the Færingehavn straight belt U-Pb zircon dating of granite sheets G85/382 and -383 (this paper) and thermobarometric evidence of 550-500°C and 5-4 kbar (Nutman and others, 1989) provides constraints on the conditions of emplacement of the QGC. Together, they show emplacement into the middle crust at ambient high to moderate temperatures, with an elevated upper crustal apparent thermal gradient of ~30°Ckm^{-1} (derived from 550-500°C and 5-4 kbar).

QÔRQUT GRANITE COMPLEX ZIRCON OXYGEN ISOTOPE SIGNATURES

Zircons from two samples of the QGC (195376 and 195392) were analysed for oxygen isotopes with SHRIMP II multi-collector by Hiess (2008) following methods described in Ickert and others (2008). Inherited Eoarchean zircon cores recorded mean $\delta^{18}O$ compositions that lie within the isotopic range of zircon in equilibrium with the Earth's mantle and likely represent tonalitic protoliths to the QGC magmas (Hiess and others, 2009). Mesoarchean and Neoarchean zircons recorded mean $\delta^{18}O$ compositions that are 0.3 to 1.3‰ lower than that of the Valley (2003) field for mantle zircon. These oscillatory zoned growth domains represent zircon that crystallized from granitic magmas formed largely by the melting of broadly tonalitic surrounding rocks, but which had previously been hydrothermally altered by meteoric water (Hiess and others, 2006, 2007). No age population from either sample demonstrates any correlation between $\delta^{18}O$ and U, Th, Th/U, common Pb or discordance systematics. This suggests that the measured oxygen isotopic ratios are primary and not a product of secondary (that is, post 2560 Ma magmatism) alteration processes (Hiess, 2008).

AEROMAGNETIC SIGNATURE

On the total-field aeromagnetic map of the Nuuk region (Rasmussen and Thorning, 1999; reproduced here as fig. 13), we have overlaid the likely southern boundary of the Kapisillik terrane, the Neoarchean Ivinnguit fault bounding the southeastern edge of the Akia terrane, the Qarliit Nunaat fault marking the northwestern extent of the Tasiusarsuaq terrane, the Færingehavn straight belt, the likely position of the poorly exposed Ivisaartoq fault and the footprint of the QGC and dated extensions of it to the southwest. Whereas in most parts of the region variation in total magnetic field is well-defined and pronounced, around the main domain of the QGC stretching from the northern reaches of inner Godthåbsfjord to between the outer parts of the fjords Ameralik and Buksefjorden in the south, there is a broad triangular domain where the variation in total magnetic field is blurred and muted. In this area the most prominent features in the aeromagnetic map are post-Qôrqut granite complex features – Palaeoproterozoic metadiabase dikes and the greenschist facies Kobbefjord fault. Therefore we propose this blurred and muted signature is related to the formation of the QGC, perhaps due to hydrothermal activity. This may be the cause of the bleaching of the country rocks, particularly prevalent at the southern steep boundary of the main part of the granite. In turn, these features might well be linked to the low $\delta^{18}O$ signature of QGC igneous zircons.

DISCUSSION

Regional syntheses for Archean crustal evolution in the Nuuk and adjacent regions

In the 1980s and 1990s, Friend, McGregor, Nutman and coworkers proposed a (tectonostratigraphic) terrane model for the Nuuk region (for example, Friend and others, 1988; McGregor and others, 1991). Windley and Garde (2009) presented a model for the Archean geological evolution of southern West Greenland Archean, in which they proposed that the Archean gneiss complex comprises *blocks* of crust formed in unrelated arc complexes of different ages, which then collided and were tilted in later tectonic movements to expose granulite-amphibolite facies crustal cross-sections. Windley and Garde (2009) and then Keulen and others (2009) presented their block model as a largely novel contribution, without clear acknowledgement that the same 3 key findings were published by us in the 1980s and 1990s, namely: (a) Crustal accretion/formation in magmatic arcs at convergent plate boundaries (for example, Nutman and others, 1989; McGregor and others, 1991), (b) collisional terrane docking and orogeny, sometimes with transient high pressure metamorphism (Friend and others, 1987 onwards) and (c) continued 'intra-continental' tectonics in laterally extensive bodies of assembled sialic crust, with folding and tilting of the earlier tectonic and metamorphic architecture (for example, "*a late Archean tilted cross section modified by deformation*.' - the first sentence in the abstract of McGregor and Friend, 1992). Thus we consider that recent independent studies by Windley and Garde (2009) support our terrane model established in the 1980s.

Although the key findings of Windley and Garde (2009) and Keulen and others (2009) confirm our work, in detail, the revised positions of their block (i.e. terrane) boundaries do not agree with available data. We take as an example the Kapisillit area (fig. 4). In the Kapisillit area, the northeastern end of the northern boundary of their Sermilik block cuts orthogonally through regional fold structures recently remapped in detail by us for the Geological Survey of Denmark and Greenland, and does not separate domains with different protolith or metamorphic histories – based on extensive U-Pb zircon and monazite dating (fig. 4; Friend and Nutman, 2005; Nutman and Friend, 2007). It also cuts orthogonally across the steep total magnetic field gradient near the edge of the Kapisillik terrane (from Rasmussen and Thorning, 1999, shown on figs. 1, 4 and 13).

Integrated model for the Qôrqut Granite Complex

Previous interpretations for the QGC (for example, McGregor, 1973; Brown and others, 1981; Friend and others, 1985) have regarded it as an essentially post-kinematic intrusion, although it was noted that its overall outcrop trend is essentially congruent with regional upright folds and rarely that QGC phases are sheared and then cut by younger non-sheared components. However, almost two decades ago, it was starting to be realised that there was major ductile shearing under lower amphibolite facies conditions that was coeval with, or outlasted, emplacement of the ~2560 Ma QGC (McGregor and others, 1991 page 192).

The available structural, geochemical, radiogenic and stable isotopic, U-Pb mineral geochronologic and aeromagnetic data (new data presented here and work cited in references given above) are integrated into a revised synthesis for the origin of the QGC. Our U-Pb zircon dating of igneous zircons from several biotite + hornblende bearing migmatite samples at deep structural levels around the northern end of the Complex supports the conclusion of Brown and others (1981) and Friend and others (1985) that the QGC is dominated by granite *sensu stricto* intrusions produced by wet melting of predominantly tonalitic orthogneisses not far below the present level of exposure in Godthåbsfjord. Finding both Mesoarchean and Eoarchean xenocrystic zircons in QGC granite sample 195376 supports the conclusion of the whole rock Pb isotopic study of Moorbath and others (1981) that the QGC source materials were a mixture of Eoarchaean and Mesoarchaean gneisses. However, in other respects, the accumulated new results lead to us revising the interpretation held in the 1970s and 1980s that the QGC is essentially a post-tectonic intrusion and that water required for the wet melting and mid-crustal levels was either from depth (mantle?) or water release from biotite and amphibole in the mid crustal source region (McGregor, 1973; Brown and others, 1981; Friend and others, 1985).

The syn-QGC regional ductile shear zones such as the Færingehavn straight belt are coaxial with broad SSW-trending non-cylindrical folds that are the latest in the region (fig. 1; McGregor and others, 1974; Chadwick and Nutman, 1979). Furthermore, mineral U-Pb dating (titanite, apatite and even locally zircon; for example, Baadsgaard and others, 1976; Nutman and Friend, 2007) indicates widespread moderately high crustal temperatures across the Nuuk region at 2600-2500 Ma, placing crustal conditions in the mostly ductile regime. Thus, emplacement of the QGC was late in the evolution of these regional folds. This is still consistent with the earlier general observations of Friend and others (1985 page 7) that '*Throughout most of its c. 150 km length the Qôrqut granite complex is orientated sub-parallel to the regional structure. However, in detail the granite complex is markedly discordant*'.

Therefore, we envisage that the QGC was emplaced into warm crust undergoing heterogeneous and perhaps intermittent deformation, with an important strike-slip component. This caused the development of the regional SSW-trending non-cylindrical folds under low pressure low amphibolite-facies metamorphic conditions, and the development of coaxial shear zones of small to large magnitudes that locally excise the limbs of these folds (Gibbs, 1976; Chadwick and Nutman, 1979). The largest proven ~2560 Ma shear zone of this type coeval with the QGC is the Færingehavn straight belt. The style of regional heterogeneous deformation gave rise to a dilational area in the Nuuk region, which was filled by repeated injection of myriads of separate granite sheets to give rise to the QGC. Because most of the QGC granite in the dilational area will be non-deformed or only weakly deformed, it has the appearance of being a post- to late-kinematic intrusion. However, away from this main locus of intrusion, such as in the Færingehavn straight belt leading from the southeastern corner of the main granite, and in the migmatites and mylonites around the northern end of the main granite, there is clearly substantial deformation that was coeval with the QGC emplacement or outlasted it.

One possible detailed geometrical solution for the emplacement of the QGC is that it occurs at a left-step on a sinistral shear zone, with the Færingehavn straight belt and Ivisaartoq fault being the offset southern and northern portions respectively (fig. 1). Within the Ivisaartoq fault at Ivisaartoq there are kinematic indicators indicating sinistral displacement, but no information is available on the Færingehavn straight belt. Upper crustal dilational fracturing, particularly above the jog, may have permitted access of meteoric water into the middle crust, where it altered the hot gneisses. We suggest this is the reason for the bleaching and blurring of lithological details in the gneisses strongest along the southwestern upper contact of the granite. Melting of these altered rocks could then give rise to the low but still positive $\delta^{18}O$ QGC igneous zircon signatures (Hiess and others, 2007, 2008). Finally, fluid ingress and circulation immediately prior to and during QGC formation might be responsible for the subdued aeromagnetic variation that occurs over the QGC and its environs (fig. 13). Another alternative model is a jog in a major dextral shear system, with the reidel shears being the dilational conduits for movement of meteoric water downwards and melt batches upwards. However, alternative kinematic models need to be tested by structural field studies, particularly the identification and interpretation of kinematic indicators.

Latest Neoarchean crustal evolution in the Nuuk and adjacent regions – a broader picture

The QGC of the Nuuk region has been the focus of this paper and several previous studies (Brown and others, 1981; Moorbath and others, 1981; Friend and others, 1985), but is neither a unique Neoarchean granite in the Archean craton of West Greenland, nor does it mark the last tectono-magmatic event. Thus zircon and monazite U-Pb dating on a deformed pegmatite sheet in the Ivinnguit fault (fig. 1) near Nuuk (sample G01/107) shows that this fault (which can be followed for at least 150 km - McGregor and others, 1991) was moving after 2535 Ma, that is, 30 million years after the emplacement of the QGC. Metamorphic conditions in the Ivinnguit fault are lowermost amphibolite to uppermost greenschist-facies. This shows that the crust was continuing to shear, and granitic pegmatites were still being produced, long after the formation of the QGC. In this case local observations on kinematic indicators show dextral movement. Furthermore on northwestern Storø (fig. 1), the amphibolite-facies dextral Storø shear zone, which is probably related to the Ivinnguit fault (Hollis and others, 2004), deforms granite and pegmatite sheets dated at ~2550 Ma (Nutman, unpublished SHRIMP U-Pb zircon data).

There is scattered reconnaissance U-Pb zircon geochronological evidence of latest Neoarchean tectono-magmatic activity throughout the West Greenland Archean craton. For example, there are metasedimentary rocks in an amphibolite facies shear zone at Kangerdluarssuk on the coast ~150 km NNW of Nuuk which have metamorphic zircons dated at 2546±6 Ma (sample G94/02 in Garde and others, 2000; inset in fig. 1) and there are granite sheets with prismatic igneous zircons giving a weighted mean $^{207}Pb/^{206}Pb$ date of 2492±11 Ma (sample 414415, table 1, inset in fig. 1), ~290 km NNW of Nuuk, near the southern margin of the Palaeoproterozoic Nagssugtoqidian orogenic belt. These sheets are variably deformed in amphibolite facies shear zones, but are cut by less deformed Kangâmiut dykes dated at ~2040 Ma (Nutman and others, 1999b). This demonstrates development of amphibolite facies shear zones and granite injection at the close of the Neoarchean. There are weakly deformed granite sheets that cut more deformed Mesoarchean orthogneisses (Nutman, unpublished U-Pb zircon data) ~300 km SSW of Nuuk at the foreland of the Paleoproterozoic Ketilidian orogen. Sample VM95/03 (inset in fig. 1) from one of these sheets collected by the 'late' V.R. McGregor yields a reconnaissance weighted mean $^{207}Pb/^{206}Pb$ age of 2540±11 Ma for prismatic igneous zircons, whereas two analyses of larger grain fragments have older ages and are interpreted as xenocrysts (sample VM95/03 in table 1).

The Nain Province in northern Labrador consists of Archean rocks once contiguous across the Davis Strait with the Archean craton in West Greenland (summary by Bridgwater and Schiøtte, 1991). In the Saglek central-northern part of the Nain Province, Baadsgaard and others (1979) obtained a U-Pb multigrain zircon age of ~2560 Ma from Neoarchean granite sheets. In the Okak central-southern portion of the Nain Province, metamorphic overgrowths on detrital zircons in an amphibolite facies metasediment from Kingnektut island has yielded a $^{207}Pb/^{206}Pb$ weighted mean age of 2562±11 Ma (Schiøtte and others, 1992).

Thus throughout the 600 km extent of the West Greenland Archean craton and once contiguous Archean crust in northern Labrador, intermittent shearing, ambient high crustal temperatures with amphibolite facies metamorphism and emplacement of crustally-derived granites occurred at the end of the Neoarchean. The low pressures for the latest Neoarchean metamorphic assemblages point to a lack of significant crustal thickening during the shearing. Also, intrusion of latest Neoarchean mafic rocks seems to be extremely rare. So far, only one reliable U-Pb date has been reported from the whole craton – a metadiabase dike from the south of Ameralik in the Nuuk region, with a baddeleyite U-Pb age of 2499±1 Ma (Nilsson, personal communication, 2009). Therefore, it would seem that the protracted latest Neoarchean shearing did not involve rampant crustal thinning (extension) either. Thus strike slip movement appears to have dominated. Granite emplacement might have been focussed at jogs on predominantly strike slip faults, where the ingress of meteoric water triggered wet melting in the crust with a generally elevated temperature. To test in detail this broad-scale model, the QGC would be the ideal target.

On the proviso that this model is correct, then the setting of this activity requires predominantly strike slip shearing, crust with an elevated average upper crustal thermal gradient of ~30°Ckm^{-1} (based on conditions of emplacement of the QGC) and production of crustally-derived granites perhaps focused at nodes of dilation and triggered by hydrous fluid fluxing. Furthermore, it should be after the last formation of magmatic arc complexes and last evidence of transient HP metamorphism related to subduction or tectonic double-thickening of older 'continental' crust. A suitable recent analogue might be the Asian continental northern hinterland of the Himalaya, where the continued northward movement of India is accommodated by long-lived 'intracontinental' tectonics, with large-scale lateral movements that partition the previously created collisional terrane architecture.

CONCLUSIONS

(1) Although the ~2560 Ma QGC post-dates terrane assembly, it is not a largely post-kinematic intrusion as previously thought, but it was coeval with low amphibolite-facies metamorphism and shear zones with important strike slip components, late in the development of regional non-cylindrical upright folds.

(2) The main body of the QGC appears to be essentially post-kinematic, only because it was emplaced in a node of dilation, during the heterogeneous predominantly strike slip deformation.

(3) Melting at this node may have been triggered by meteoric water peculating down dilational fractures, causing alteration of the crust – focussed at the brittle-ductile transition. Melting of these altered rocks gave rise to the low $\delta^{18}O$ signature of QGC igneous zircons (Hiess and others, 2007, 2008).

(4) Due to the hydrous nature of the melting event, the QGC was emplaced immediately above its migmatitic generation zone.

(5) Shearing and pegmatite emplacement continued to at least 2530 Ma in the Nuuk region, as shown by dating of a deformed granite sheet in the Ivinnguit fault. Furthermore, this activity is not unique to the Nuuk region, but occurs throughout the ~600 km extent of the West Greenland Archean craton.

(6) A suitable recent analogue for the 'intracratonic' latest Neoarchean events in West Greenland might be the northern hinterland of the Himalayas, where there is far-field, long-lived accommodation of Asian crust due to the continued northern movement of India.

ACKNOWLEDGMENTS

Work was supported by the Geological Survey of Denmark and Greenland , NERC (U.K.) grant NER/A/S/1999/00024 and ARC (Australia) grant DP0342798. Joe Hiess was supported by APA and Jaeger scholarships while a Ph.D. student at the Australian National University. Funding to support APN from the Chinese Academy of Geological Sciences is acknowledged. The Geological Survey of Denmark and Greenland is thanked for permission to publish this paper and to reproduce the aeromagnetic data shown in figure 13.

APPENDIX

Analytical protocols generally follow those given by Stern (1998) and Williams (1998). Some samples were analysed in the previous millennium without pre-analysis cathodoluminescence (CL) imaging to guide the choice of analytical sites. In all such cases, retrospective CL imaging was undertaken in the present millennium, sometimes with additional analyses, and the data re-assessed. Many of the zircons in granites and pegmatites have high U (and sometimes Th) contents, meaning that by counting statistics alone, they would often have very small analytical errors on their $^{207}Pb/^{206}Pb$ ratios, equivalent to only 1 or 2 Ma (1σ). Given that many of the high U sites show internal variations in ^{207}Pb and ^{206}Pb count rates well beyond that expected from the total counts alone, this extra 'noise' was added-in in quadrature, to ensure a more realistic assessment of the precision of $^{207}Pb/^{206}Pb$ measurement.

The monazites were calibrated with analyses of the Thompson mine monazite standard (average $^{206}Pb/^{238}U$ age = 1760 Ma, average U content of 2100 ppm). The monazites were analysed on SHRIMP 1, but without retardation of the secondary beam in front of the electron multiplier, and a small isobaric interference under ^{204}Pb was not filtered-out. Therefore, the $^{207}Pb/^{206}Pb$ age corrected using measured mass 204 will be slightly overcorrected for common Pb.

REFERENCES

Baadsgaard, H., 1976, Further U-Pb dates on zircons from the early Precambrian rocks of the Godthaabsfjord area, West Greenland: Earth and Planetary Science Letters, v. 33, p. 261-267.

Baadsgaard, H., Lambert, R. St. J., and Krupicka, J., 1976, Mineral isotopic age relationships in the polymetamorphic Amitsoq gneisses, Godthaab District, West Greenland. Geochimica et Cosmochimica Acta, v. 40, 513-528.

Baadsgaard, H., Collerson, K.D., and Bridgwater, D., 1979, The Archaean gneiss complex of northern Labrador. 1. Preliminary U-Th-Pb geochronology: Canadian Journal of Earth Sciences, v. 16, p. 951-961.

Bennett, V.C., Nutman, A.P., and McCulloch, M.T., 1993, Nd isotopic evidence for transient, highly depleted mantle reservoirs in the early history of the Earth: Earth and Planetary Science Letters, v. 119, p. 299-317.

Berthelsen, A., 1960, Structural studies in the pre-Cambrian of western Greenland. II. Geology of Tovqussaq nunâ: Bulletin Grønlands Geologiske Undersøgelse, v. 25, 223 pp.

Black, L.P., Gale, N.H., Moorbath, S., Pankhurst, R.J., and McGregor, V.R., 1971, Isotopic dating of very early Precambrian amphibolite facies gneisses from the Godthåb district, West Greenland: Earth and Planetary Science Letters. v. 12, p. 245-259.

Bridgwater, D., and Schiøtte, L., 1991, The Archaean gneiss complex of northern Labrador. A review of current results, ideas and problems: Bulletin of the Geological Society of Denmark, v. 39, p. 153-166.

Bridgwater, D., McGregor, V.R., and Myers, J.S., 1974, A horizontal tectonic regime in the Archaean of Greenland and its implications for early crustal thickening: Precambrian Research, v. 1, p. 179-197.

Brown, M., Friend, C.R.L., McGregor, V.R., and Perkins, W.T., 1981, The late Archaean Qôrqut granite complex of southern West Greenland: Journal of Geophysical Research, v. 86, p. 10617-10632.

Chadwick, B., and Nutman, A.P., 1979, Archaean structural evolution in the northwest of the Buksefjorden region, southern West Greenland: Precambrian Research, v. 9, p. 199-226.

Coney, P.J., Jones, D.L., and Monger, J.W.H., 1980, Cordilleran suspect terranes: Nature, v. 288, p. 329-333.

Crowley, J.L., 2002, Testing the model of late Archean terrane accretion in southern West Greenland: a comparison of timing of geological events across the Qarliit Nunaat fault, Buksefjorden region: Precambrian Research, v. 116, p. 57-79.

Cumming, G.L., and Richards, J.R., 1975, Ore lead ratios in a continuously changing Earth: Earth and Planetary Science Letters, v. 28, p. 155-171.

Dymek, R.F., 1983, Margarite pseudomorphs after corundum, Qôrqut area, Godthåbsfjord, West Greenland: Rapport Grønlands geologiske Undersøgelse, v. 112, p. 95-99.

Friend, C.R.L., and Hall, R.P.H., 1977, Fieldwork on the Ivisârtoq area, inner Godthåbsfjord, southern West Greenland: Grønlands Geologiske Undersøgelse Rapport, v. 85, p. 54-60.

Friend, C.R.L., and Nutman, A.P., 2001, U-Pb zircon study of tectonically-bounded blocks of 2940-2840 Ma crust with different metamorphic histories, Paamiut region, South-West Greenland: Implications for the tectonic assembly of the North Atlantic craton: Precambrian Research, v. 105, p. 143-164.

Friend, C.R.L., and Nutman, A.P., 2005, New pieces to the Archaean terrane jigsaw puzzle in the Nuuk region, southern West Greenland: Steps in transforming a simple insight into a complex regional tectonothermal model: Journal of the Geological Society of London, v. 162, p. 147-163.

Friend, C.R.L., Brown, M., Perkins, W.T., and Burwell, A.D.M., 1985, The geology of the Qôrqut Granite Complex north of Qôrqut, Godthåbsfjord, southern West Greenland: Bulletin of Grønlands geologiske Undersøgelse, v. 151, 43 pp.

Friend, C.R.L., Nutman, A.P., and McGregor, V.R., 1987, Late-Archaean tectonics in the Færingehavn–Tre Brødre area, south of Buksefjorden, southern West Greenland: Journal of the Geological Society of London, v. 144, p. 369-376.

Friend, C.R.L., Nutman, A.P., and McGregor, V.R., 1988, Late Archaean terrane accretion in the Godthåb region, southern West Greenland: Nature, v. 335, p. 535-538.

Friend, C.R.L., Nutman, A.P., Baadsgaard, H., Kinny, P.D., and McGregor, V.R., 1996, Timing of late Archaean terrane assembly, crustal thickening and granite emplacement in the Nuuk region, southern West Greenland: Earth and Planetary Science Letters, v. 124, p. 353-365.

Friend, C.R.L., Nutman, A.P., Baadsgaard, H., and Duke, J.M., 2009, The whole rock Sm-Nd ‘age’ for the 2825 Ma Ikkattoq gneisses (Greenland) is 800 Ma too young: Insights into Archaean TTG petrogenesis: Chemical Geology, v. 261, p. 62-76.

Garde, A.A., Friend, C.R.L., Nutman, A.P., and Marker, M., 2000, Rapid maturation and stabilisation of middle Archaean continental crust: the Akia terrane, southern West Greenland: Bulletin of the Geological Society of Denmark, v. 47, p. 1–27.

Garde, A.A., 2007, A mid-Archaean island arc complex in the eastern Akia terrane, Godthåbsfjord, southern West Greenland: Journal of the Geological Society of London, v. 164, p. 565-579.

Gibbs, A.D., 1976, Structural studies in part of the Buksefjorden region, south west Greenland: PhD Thesis, University of Exeter, U.K.

Griffin, W.L., McGregor, V.R., Nutman, A.P., Taylor, P.N., and Bridgwater, D., 1980, Early Archaean granulite-facies metamorphism south of Ameralik: Earth and Planetary Science Letters, v. 50, p. 59-74.

Hiess J., 2008, Early Crustal Petrogenesis: Integrated in situ U-Pb, O, Hf and Ti isotopic systematics of zircon from Archaean rocks, West Greenland: Unpublished Ph.D. thesis, The Australian National University, Canberra, 280pp.

Hiess J., Bennett V. C., Nutman A. P., and Williams I. S., 2007, In situ Hf and O isotopic data from Archean zircons of SW Greenland: Geochimica et Cosmochimica Acta, v. 71, 15, A404. Goldschmidt Conference, Cologne, Germany.

Hiess J., Bennett V., Nutman A., Williams I. S., and Eggins S., 2008, Archean TTG petrogenesis – The U/Pb-O-Hf isotopic perspective: Geochimica et Cosmochimica Acta, v. 72, 12, A375. Goldschmidt Conference, Vancouver, Canada.

Hiess J., Bennett V. C., Nutman A. P., and Williams I. S., 2009, In situ U-Pb, O and Hf isotopic compositions of zircon from Eoarchaean rocks, West Greenland: New insights to making old crust: Geochimica et Cosmochimica Acta, v. 73, p. 4489-4516.

Hollis, J.A., Frei, D., van Gool, J.A.M., Garde, A.A., and Persson, M., 2005, Using zircon geochronology to resolve the Archaean geology of southern West Greenland: Bulletin of the Geological Survey of Denmark and Greenland, v. 10, p. 49-52.

Horie, K., Nutman, A.P., Friend, C.R.L., and Hidaka, H., in press, The complex age of orthogneiss protoliths exemplified by the Eoarchaean Itsaq Gneiss Complex (Greenland): SHRIMP and old rocks: Precambrian Research (accepted for publication, July 2010).

Ickert R. B., Hiess J., Williams I. S., Holden P., Ireland T. R., Lanc P., Schram N., Foster J. J., and Clement S. W., 2008, Determining high precision, in situ, oxygen isotope ratios with a SHRIMP II: analyses of MPI- DING silicate-glass reference materials and zircon from contrasting granites: Chemical Geology, v. 257, p. 114–128.

Keulen, N., Scherstén, A., Schumacher, J.C., Næraa, T., and Windley, B.F., 2009, Geological observations in the southern West Greenland basement from Ameralik to Frederikshåb Isblink in 2008: Geological Survey of Denmark and Greenland Bulletin, v. 17, p. 49-52.

Kinny, P.P., 1986, 3820 Ma zircons from tonalitic Amîtsoq gneiss in the Godthåb district of southern West Greenland: Earth and Planetary Science Letters, v. 79, p. 337-347.

Ludwig, K., 1998, Using ISOPLOT/EX Version 1.00b: a geochronological toolkit for Microsoft Excel: Berkeley Geochronology Center, Spec. Publ. 1.

McGregor, V.R., 1973, The early Precambrian gneisses of the Godthåb district, West Greenland: Philosophical Transactions of the Royal Society, London, v. A273, p. 343-358.

McGregor, V.R., 1979, Archean gray gneisses and the origin of the continental crust: evidence from the Godthåb region, West Greenland: In: F. Barker (Editor), Trondhjemites, dacites and related rocks. Developments in Petrology, v. 6, Elsevier, Amsterdam, p. 169-204.

McGregor, V.R., and Friend, C.R.L., 1992, Late Archaean prograde amphibolite- to granulite-facies relations in the Fiskenæsset region, southern West Greenland: Journal of Geology, v. 100, p. 207-219.

McGregor, V.R., Friend, C.R.L., and Nutman, A.P., 1991, The late Archaean mobile belt through Godthåbsfjord, southern West Greenland: a continent-continent collision zone?: Bulletin of the Geological Society of Denmark, v. 39, p. 179-197.

Moorbath, S., and Pankhurst, R.J., 1976, Further rubidium-strontium age and isotope evidence for the nature of the late Archaean plutonic event in West Greenland: Nature, v. 262, p. 124-126.

Moorbath, S., O'Nions, R.K., Pankhurst, R.J., Gale, N.H., and McGregor, V.R., 1972, Further rubidium-strontium age determinations on the very early Precambrian rocks of the Godthåb district: West Greenland: Nature, v. 240, p. 78-82.

Moorbath, S. Taylor, P.N., and Goodwin, R., 1981, Origin of granitic magma by crustal remobilisation: Rb-Sr and Pb/Pb geochronology and isotope geochemistry of the late Archaean Qôrqut Granite Complex of southern West Greenland: Geochimica et Cosmochimica Acta, v. 45, p. 1051-1060.

Moorbath, S, Taylor, P.N., and Jones, N.W., 1986, Dating the oldest terrestrial rocks – fact and fiction: Chemical Geology, v. 57, p. 63-86.

Nutman, A.P., and Friend, C.R.L., 2007, Adjacent terranes with c. 2715 and 2650 Ma high-pressure metamorphic assemblages in the Nuuk region of the North Atlantic Craton, southern West Greenland: Complexities of Neoarchaean collisional orogeny: Precambrian Research, v. 155, p. 159-203.

Nutman, A.P., Friend, C.R.L., and McGregor, V.R., 1988, Reappraisal of the geology of Kangimut sammissoq, Ameralik Fjord, southern West Greenland: crustal structure and the interpretation of isotopic data: In: Ashwal, L. (Editor) Workshop on the growth of Continental Crust, LPI Tech. Rept., v. 88-02, pp. 112-115.

Nutman, A.P., Friend, C.R.L., Baadsgaard, H., and McGregor, V.R., 1989, Evolution and assembly of Archean gneiss terranes in the Godthåbsfjord region, southern West

Greenland: Structural, metamorphic, and isotopic evidence: Tectonics, v. 8, p. 573-589.

Nutman, A.P., McGregor, V.R., Friend, C.R.L., Bennett, V.C., and Kinny, P.D., 1996, The Itsaq Gneiss Complex of southern West Greenland; the world's most extensive record of early crustal evolution (3900-3600 Ma): Precambrian Research, v. 78, p. 1-39.

Nutman, A.P., Bennett, V.C., Friend, C.R.L., and Norman, M., 1999a, Meta-igneous (non-gneissic) tonalites and quartz-diorites from an extensive ca. 3800 Ma terrain south of the Isua supracrustal belt, southern West Greenland: Constraints on early crust formation: Contributions to Mineralogy and Petrology, v. 137, p. 364-388.

Nutman, A.P., Kalsbeek, K., Marker, M., van Gool, J.A.M., and Bridgwater, D., 1999b, U-Pb zircon ages of Kangâmiut dykes and detrital zircons in the Palaeoproterozoic Nagssugtoqidian Orogen (West Greenland): Clues to the pre-collisional history of the orogen: Precambrian Research, v. 93, p. 87-104.

Nutman, A.P., Friend, C.R.L., Barker, S.S., and McGregor, V.R., 2004, Inventory and assessment of Palaeoarchaean gneiss terrains and detrital zircons in southern West Greenland: Precambrian Research, v. 135, p. 281-314.

Nutman, A.P., Christiansen, O., and Friend, C.R.L., 2007, 2635-2610 Ma structurally controlled lode-gold mineralisation near a terrane boundary (suture?) at Storø, Nuuk region, southern West Greenland: Precambrian Research, v. 159, p. 19-32.

Nutman, A.P., Bennett, V.C., Friend, C.R.L., Jenner, F., Wan, Y., and Liu, D.Y., 2009, Eoarchaean crustal growth in West Greenland (Itsaq Gneiss Complex) and in northeastern China (Anshan area): review and synthesis. In: P. Cawood and A. Kröner (Editors), Earth Accretionary Systems in Space and Time: Special Publications of the Geological Society, v. 318, p. 127-154.

O'Brien, P.J., and Rötzler, J., 2003, High-pressure granulites: formation, recovery of peak conditions and implications for tectonics: Journal of Metamorphic Petrology, v. 21, p. 3-20.

Pattison, D.R.M., 2003, Petrogenetic significance of orthopyroxene-free garnet + clinopyroxene + plagioclase ± quartz-bearing metabasites with respect to the amphibolite and granulite facies: Journal of Metamorphic Petrology, v. 21, p. 21-34.

Polat, A., Frei, R., Appel, P.W.U., Dilek, Y., Fryer, B., Ordóñez-Calderón, J.C., and Yang, Z., 2008, The origin and compositions of Mesoarchean oceanic crust: Evidence from the 3075 Ma Ivisaartoq greenstone belt, SW Greenland: Lithos, v. 100, p. 293-321.

Rasmussen, T.M., and Thorning, L., 1999, Airborne geophysical surveys in Greenland in 1998: Geology of Greenland Survey Bulletin, v. 183, p. 34-38.

Rollinson, H., 2003, Metamorphic history suggested by garnet-growth chronologies in the Isua Greenstone Belt, West Greenland: Precambrian Research, v. 126, p. 181-196.

Schiøtte, L., Compston, W., and Bridgwater, D., 1988, Late Archaean ages for the deposition of clastic sediments belonging to the Malene supracrustals, southern West Greenland: Evidence from an ion probe U-Pb zircon study: Earth and Planetary Science Letters, v. 87, p. 45-58.

Schiøtte, L., Compston, W., and Bridgwater, D., 1989, U-Pb single zircon age for the Tinissaq gneiss of southern West Greenland: A controversy resolved: Chemical Geology, v. 79, p. 21-30.

Schiøtte, L., Nutman, A.P., and Bridgwater, D., 1992, U-Pb ages of single zircons within "Upernavik" metasedimentary rocks and regional implications for the tectonic evolution of the Archaean Nain Province, Labrador: Canadian Journal of Earth Sciences, v. 29, p. 260-276.

Sharpe, M.R., 1975, Anorthosites and serpentinites of the Færingehavn area, southern West Greenland, and their position in the regional chronology: PhD Thesis, University of Exeter, U.K.

Steenfelt, A., Garde, A.A., and Moyen, J.F., 2005, Mantle wedge involvement in the petrogenesis of Archaean grey gneisses in West Greenland: Lithos, v. 79, p. 207–228.

Stern, R.A., 1998, High-resolution SIMS determination of radiogenic trace-isotope ratios in minerals. In L. J. Cabri and D.J. Vaughan (Editors). Modern approaches to ore and environmental mineralogy. Mineralogical Association of Canada Short Course Series, 27, 241-268.

Valley, J., 2003, Oxygen isotopes in zircon. In J.M. Hanchar and P.W.O. Hoskin (Editors). Zircon: Reviews in Mineralogy and Geochemistry, v. 53, p. 343-385.

Wells, P.R.A., 1976, Late Archaean metamorphism in the Buksefjorden region of southern West Greenland: Contributions to Mineralogy and Petrology, v. 56, p. 229-242.

Windley, B.F., and Garde, A.A., 2009, Arc-generated blocks with crustal sections in the North Atlantic craton of West Greenland: Crustal growth in the Archean with modern analogues: Earth Sciences Reviews, v. 93, p.1-30.

Williams, I.S., 1998, U-Th-Pb geochronology by ion microprobe. In: M.A. McKibben, W.C.P. Shanks III and W.I. Ridley (Editors). Applications of microanalytical techniques to understanding mineralizing processes. Soc. Econ. Geol. Short Course Vol. 7.

Williams, I.S., Compston, W., Black, L.P., Ireland, T.R., and Foster, J.J., 1984, Unsupported radiogenic Pb in zircon: a case of anomalously high Pb-Pb, U-Pb and Th-Pb ages: Contributions to Mineralogy and Petrology, v. 88, p. 322-327.

Table caption

Table 1. SHRIMP U-Pb zircon and monazite analytical data.

Figure captions

Figure 1. Geological map of the Nuuk region. In the bottom right inset *Nag* is the southern boundary of the Paleoproterozoic Nagssugtoqidian orogen and *Ket* is the northern boundary of the Paleoproterozoic Ketilidian orogen. The bottom left inset gives the ages of juvenile crustal components (predominantly tonalites) in the Nuuk region terranes.

Figure 2. Geological map of the Færingehavn area, based on mapping by Friend and Nutman. Previously-published geochronology is from Bennett and others (1993), Crowley (2002), Nutman and Friend (2007), Friend and others (2009), Nutman and others (2009).

Figure 3. Timeline, with compiled <3900 Ma dates for different terranes and events common to them after assembly, based on U-Pb zircon and monazite geochronology. Dates are from this paper, Crowley (2002); Friend and others (1996); Friend and Nutman (2001, 2005); Garde (2007), Garde and others (2000), Nutman and Friend (2007), Nutman and others (1999a, 2002, 2004, 2007).

Figure 4. Geological map of the Kapisillit area, largely based on mapping by Friend and Nutman.

Figure 5. (A) 800 m vertical exposure approximately 5 km northwest of Qooqqut, Godthåbsfjord, showing intrusion of myriads of QGC granite sheets at essentially the same crustal level within the middle to upper levels of the complex. (B) 500 m vertical exposure of the top part of the 1493 m mountain approximately 8 km north of Qooqqut, showing intrusion of gently inclined of QGC pegmatite sheets in the upper zone of the complex.

Figure 6. ^{207}Pb/^{206}Pb versus ^{238}U/^{206}Pb plots of zircon analyses of granite sample 195376 from the main body of the QGC (see fig. 1 for locality). (A) all analyses of

igneous and xenocrystic zircon. (B) analyses of igneous zircons. Analytical errors are depicted at the 2σ level.

Figure 7. Representative images of zircons and a monazite. All are cathodoluminescence images, apart from those marked ‘TL’ which are transmitted light images. All grains are shown at the same scale, apart from G01/107 large monazite grain 1 which is reduced in size 50%. Marked ages are $^{207}Pb/^{206}Pb$ ages (Ma), with 2σ analytical errors. Due to space considerations, the multiple age determinations on G01/107 monazite grain are not shown (see table 1). (A) Strongly deformed granite sheet within the fabric of the Færingehavn straight belt. (B) weakly deformed granite sheet discordant to the fabric of the Færingehavn straight belt. (C) migmatite 195392 at a deep structural level in the QGC. (D) deformed granite sheet cutting mylonites in the Ivinnguit fault.

Figure 8. $^{207}Pb/^{206}Pb$ versus $^{238}U/^{206}Pb$ plots of zircon analyses of granite sheets from the islet Smukke Ø south of Færingehavn. (A) G85/282 strongly deformed granite concordant within the Færingehavn straight belt fabric. (B) G85/283 weakly deformed granite discordant to the Færingehavn straight belt fabric. Analytical errors are depicted at the 2σ level.

Figure 9. Sampling localities of migmatites (A) 430115 (pen for scale top-middle of view) and (B) 481415 (field of view ~ 1 m; see Fig. 4 for localities).

Figure 10. $^{207}Pb/^{206}Pb$ versus $^{238}U/^{206}Pb$ plots of zircon analyses. (A) migmatite 480115, (B) migmatite 481415, (C) migmatite 195392 and (D) granite lithon 459809 in mylonite. Analytical errors are depicted at the 2σ level.

Figure 11. Sampling locality of variably deformed granite sheets in mylonite, west of Itinera (see fig. 4 for localities). (A) granite lithon in mylonite, sample 459809. (B) discordant but deformed granite sheet 459808 cutting mylonite. Pen for scale in both images.

Figure 12. ^{207}Pb/^{206}Pb versus ^{238}U/^{206}Pb plots of (A) zircon analyses and (B) monazite analyses from variably deformed granite sheet G01/107 within the Ivinnguit fault, near Nuuk (see fig. 1 for locality). Analytical errors are depicted at the 2σ level.

Figure 13. Total magnetic field aeromagnetic map of the Nuuk region (after Rasmussen and Thorning, 1999; reproduced here with permission of the Geological Survey of Denmark and Greenland).

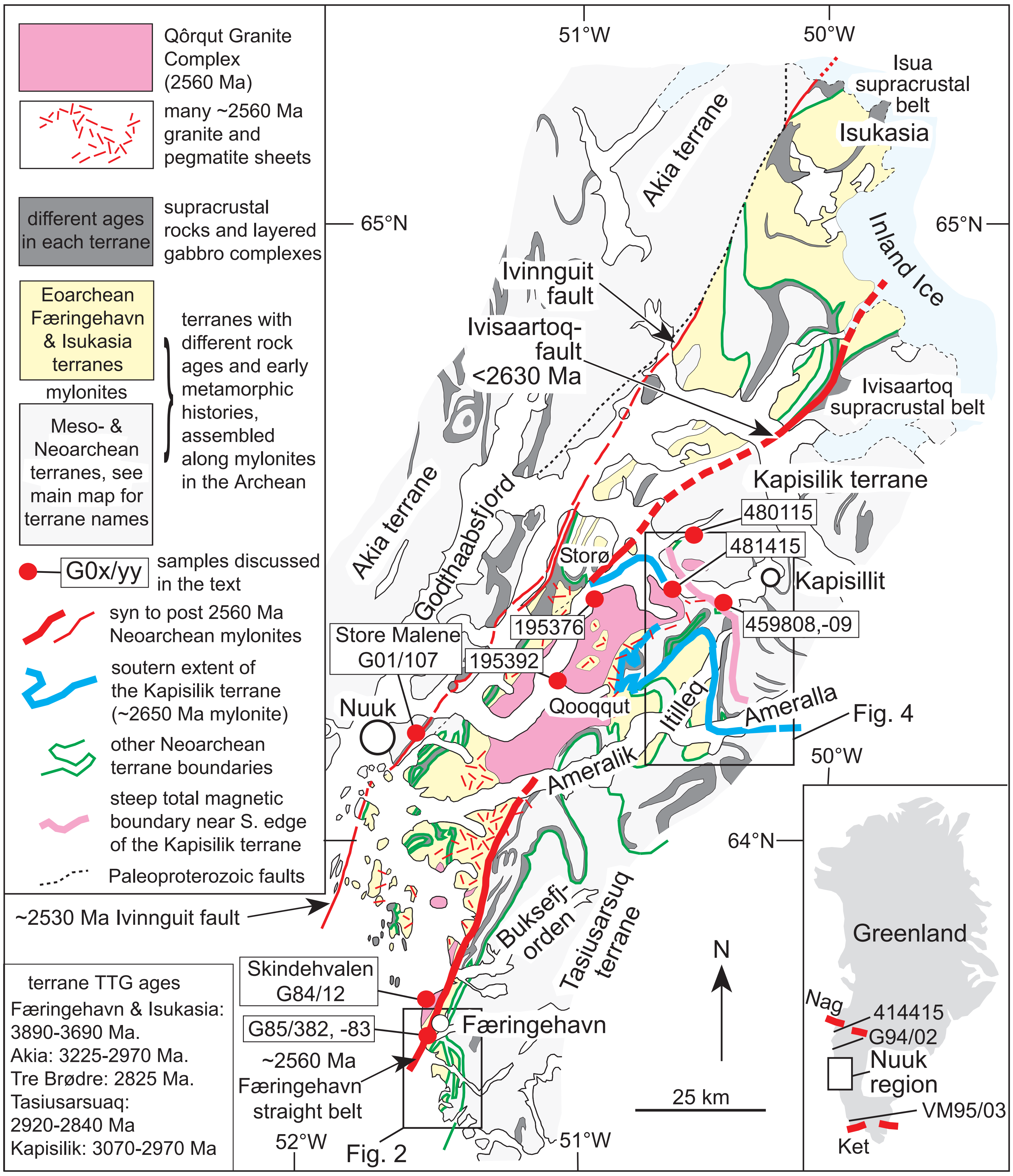

Qôrqut Granite Complex (2560 Ma)
many ~2560 Ma granite and pegmatite sheets
different ages in each terrane
supracrustal rocks and layered gabbro complexes
Eoarchean Færingehavn & Isukasia terranes
mylonites
Meso- & Neoarchean terranes, see main map for terrane names
terranes with different rock ages and early metamorphic histories, assembled along mylonites in the Archean
G0x/yy
samples discussed in the text
syn to post 2560 Ma Neoarchean mylonites
soutern extent of the Kapisilik terrane (~2650 Ma mylonite)
other Neoarchean terrane boundaries
steep total magnetic boundary near S. edge of the Kapisilik terrane
Paleoproterozoic faults
~2530 Ma Ivinnguit fault
terrane TTG ages
Færingehavn & Isukasia: 3890-3690 Ma.
Akia: 3225-2970 Ma.
Tre Brødre: 2825 Ma.
Tasiusarsuaq: 2920-2840 Ma
Kapisilik: 3070-2970 Ma
51°W
50°W
65°N
Isua supracrustal belt
Isukasia
Akia terrane
Inland Ice
Ivinnguit fault
Ivisaartoq-fault <2630 Ma
Ivisaartoq supracrustal belt
Kapisilik terrane
Akia terrane
Godthaabsfjord
480115
481415
Storø
Kapisillit
195376
459808,-09
Store Malene G01/107
195392
Nuuk
Qooqqut
Itilleq
Ameralla
Fig. 4
50°W
Ameralik
64°N
Buksefj-orden
Tasiusarsuaq terrane
Greenland
Nag
414415
G94/02
Nuuk region
VM95/03
Ket
N
25 km
Skindehvalen G84/12
G85/382, -83
Færingehavn
~2560 Ma Færingehavn straight belt
52°W
Fig. 2
51°W

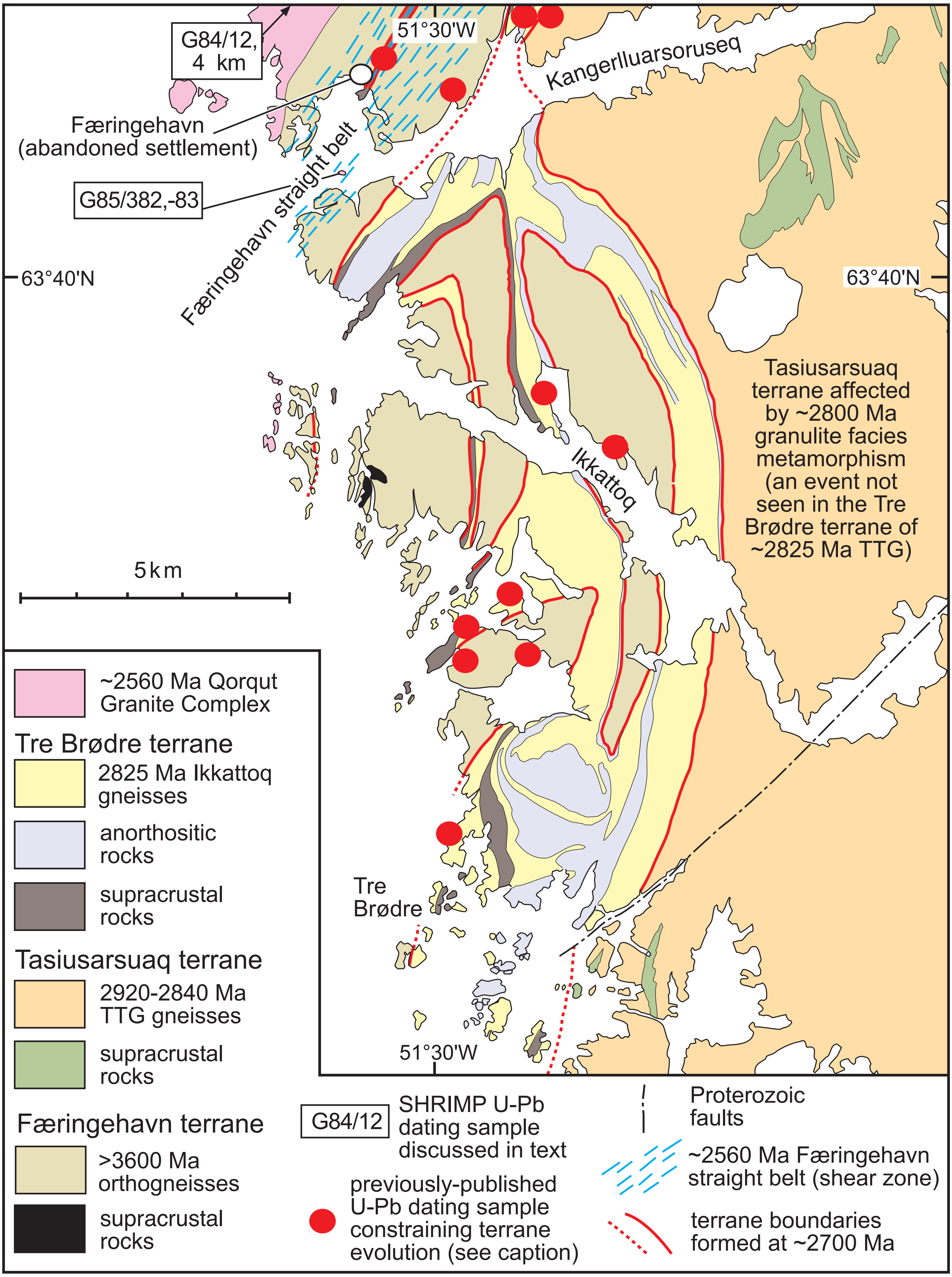

G84/12,
4 km
51°30'W
Kangerlluarsoruseq
Færingehavn
(abandoned settlement)
Færingehavn straight belt
G85/382,-83
63°40'N
63°40'N
Tasiusarsuaq terrane affected by ~2800 Ma granulite facies metamorphism (an event not seen in the Tre Brødre terrane of ~2825 Ma TTG)
Ikkattoq
5 km
Tre Brødre
51°30'W
~2560 Ma Qorqut Granite Complex
Tre Brødre terrane
2825 Ma Ikkattoq gneisses
anorthositic rocks
supracrustal rocks
Tasiusarsuaq terrane
2920-2840 Ma TTG gneisses
supracrustal rocks
Færingehavn terrane
>3600 Ma orthogneisses
supracrustal rocks
G84/12
SHRIMP U-Pb dating sample discussed in text
previously-published U-Pb dating sample constraining terrane evolution (see caption)
Proterozoic faults
~2560 Ma Færingehavn straight belt (shear zone)
terrane boundaries formed at ~2700 Ma

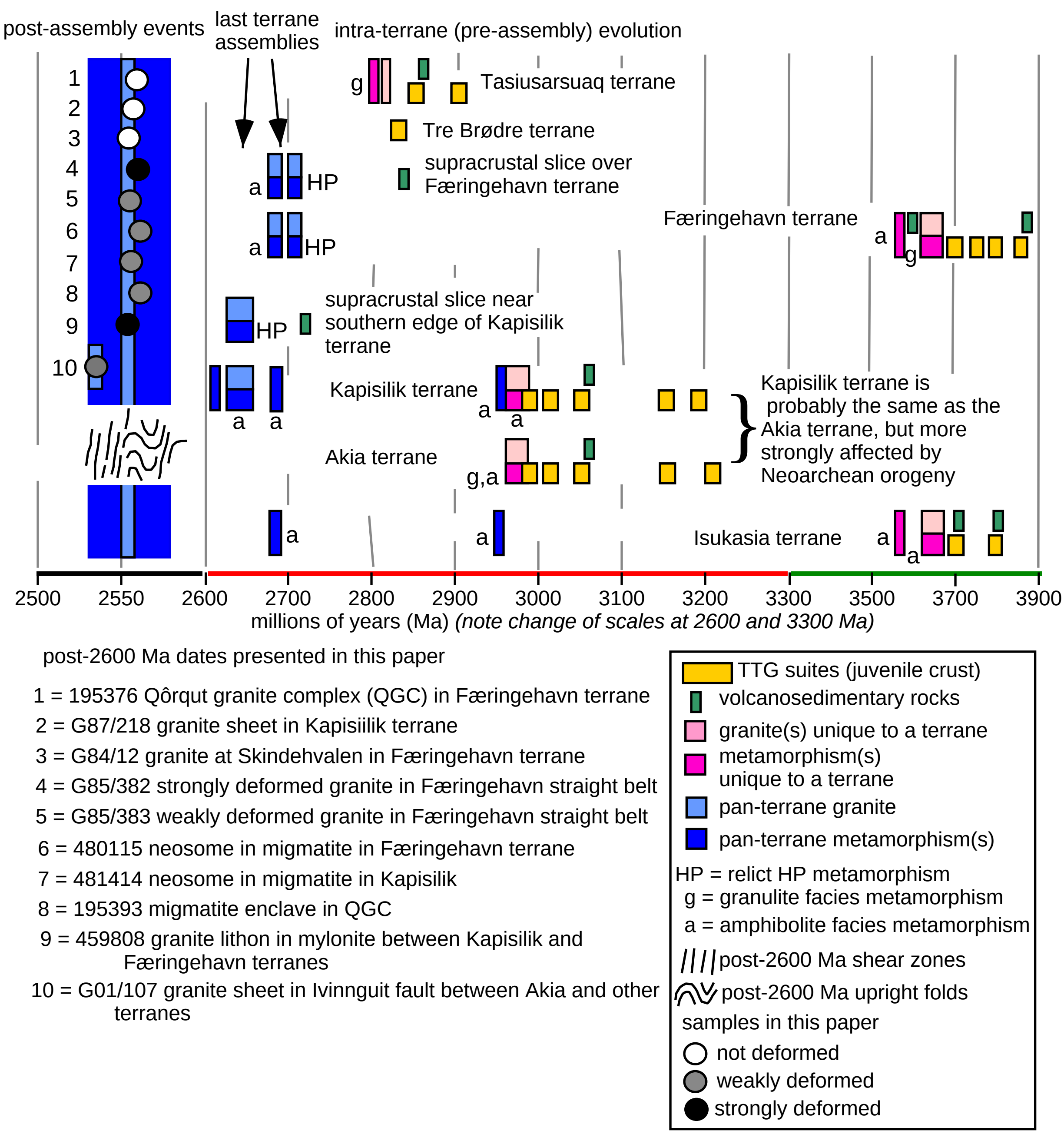
post-assembly events
last terrane assemblies
intra-terrane (pre-assembly) evolution
1
2
3
4
5
6
7
8
9
10
Tasiusarsuaq terrane
Tre Brødre terrane
supracrustal slice over Færingehavn terrane
Færingehavn terrane
supracrustal slice near southern edge of Kapisilik terrane
Kapisilik terrane
Akia terrane
Kapisilik terrane is probably the same as the Akia terrane, but more strongly affected by Neoarchean orogeny
Isukasia terrane
HP
a
g
g,a
2500
2550
2600
2700
2800
2900
3000
3100
3200
3300
3500
3700
3900
millions of years (Ma) *(note change of scales at 2600 and 3300 Ma)*
post-2600 Ma dates presented in this paper
1 = 195376 Qôrqut granite complex (QGC) in Færingehavn terrane
2 = G87/218 granite sheet in Kapisiilik terrane
3 = G84/12 granite at Skindehvalen in Færingehavn terrane
4 = G85/382 strongly deformed granite in Færingehavn straight belt
5 = G85/383 weakly deformed granite in Færingehavn straight belt
6 = 480115 neosome in migmatite in Færingehavn terrane
7 = 481414 neosome in migmatite in Kapisilik
8 = 195393 migmatite enclave in QGC
9 = 459808 granite lithon in mylonite between Kapisilik and Færingehavn terranes
10 = G01/107 granite sheet in Ivinnguit fault between Akia and other terranes
TTG suites (juvenile crust)
volcanosedimentary rocks
granite(s) unique to a terrane
metamorphism(s) unique to a terrane
pan-terrane granite
pan-terrane metamorphism(s)
HP = relict HP metamorphism
g = granulite facies metamorphism
a = amphibolite facies metamorphism
post-2600 Ma shear zones
post-2600 Ma upright folds
samples in this paper
not deformed
weakly deformed
strongly deformed

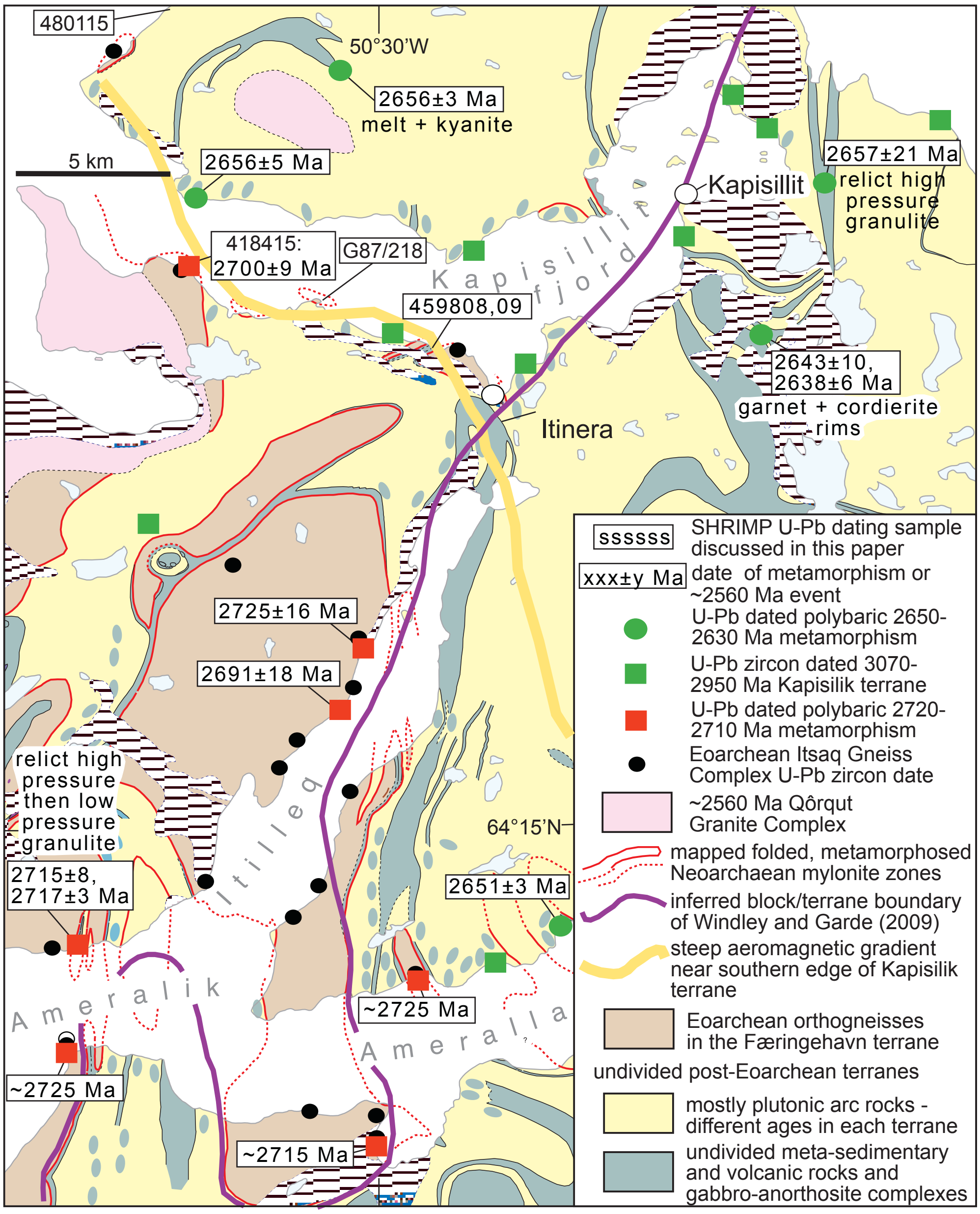

480115
50°30'W
2656±3 Ma
melt + kyanite
5 km
2656±5 Ma
418415:
2700±9 Ma
G87/218
Kapisillit fjord
459808,09
Kapisillit
2657±21 Ma
relict high pressure granulite
2643±10,
2638±6 Ma
garnet + cordierite rims
Itinera
2725±16 Ma
2691±18 Ma
relict high pressure then low pressure granulite
2715±8,
2717±3 Ma
Itilleq
Ameralik
~2725 Ma
~2715 Ma
~2725 Ma
Ameralla
64°15'N
2651±3 Ma
ssssss SHRIMP U-Pb dating sample discussed in this paper
xxx±y Ma date of metamorphism or ~2560 Ma event
U-Pb dated polybaric 2650-2630 Ma metamorphism
U-Pb zircon dated 3070-2950 Ma Kapisilik terrane
U-Pb dated polybaric 2720-2710 Ma metamorphism
Eoarchean Itsaq Gneiss Complex U-Pb zircon date
~2560 Ma Qôrqut Granite Complex
mapped folded, metamorphosed Neoarchaean mylonite zones
inferred block/terrane boundary of Windley and Garde (2009)
steep aeromagnetic gradient near southern edge of Kapisilik terrane
Eoarchean orthogneisses in the Færingehavn terrane
undivided post-Eoarchean terranes
mostly plutonic arc rocks - different ages in each terrane
undivided meta-sedimentary and volcanic rocks and gabbro-anorthosite complexes


A
B

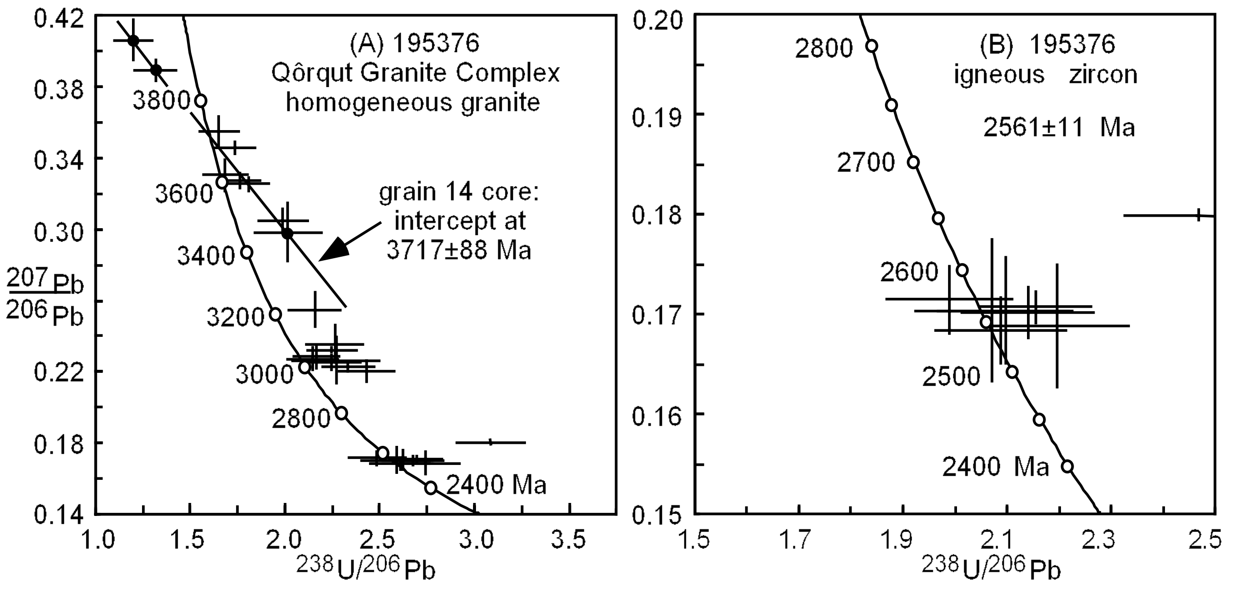

(A) 195376
Qôrqut Granite Complex
homogeneous granite
grain 14 core:
intercept at
3717±88 Ma
3800
3600
3400
3200
3000
2800
2400 Ma
$^{207}Pb/^{206}Pb$
$^{238}U/^{206}Pb$
(B) 195376
igneous zircon
2561±11 Ma
2800
2700
2600
2500
2400 Ma
$^{238}U/^{206}Pb$

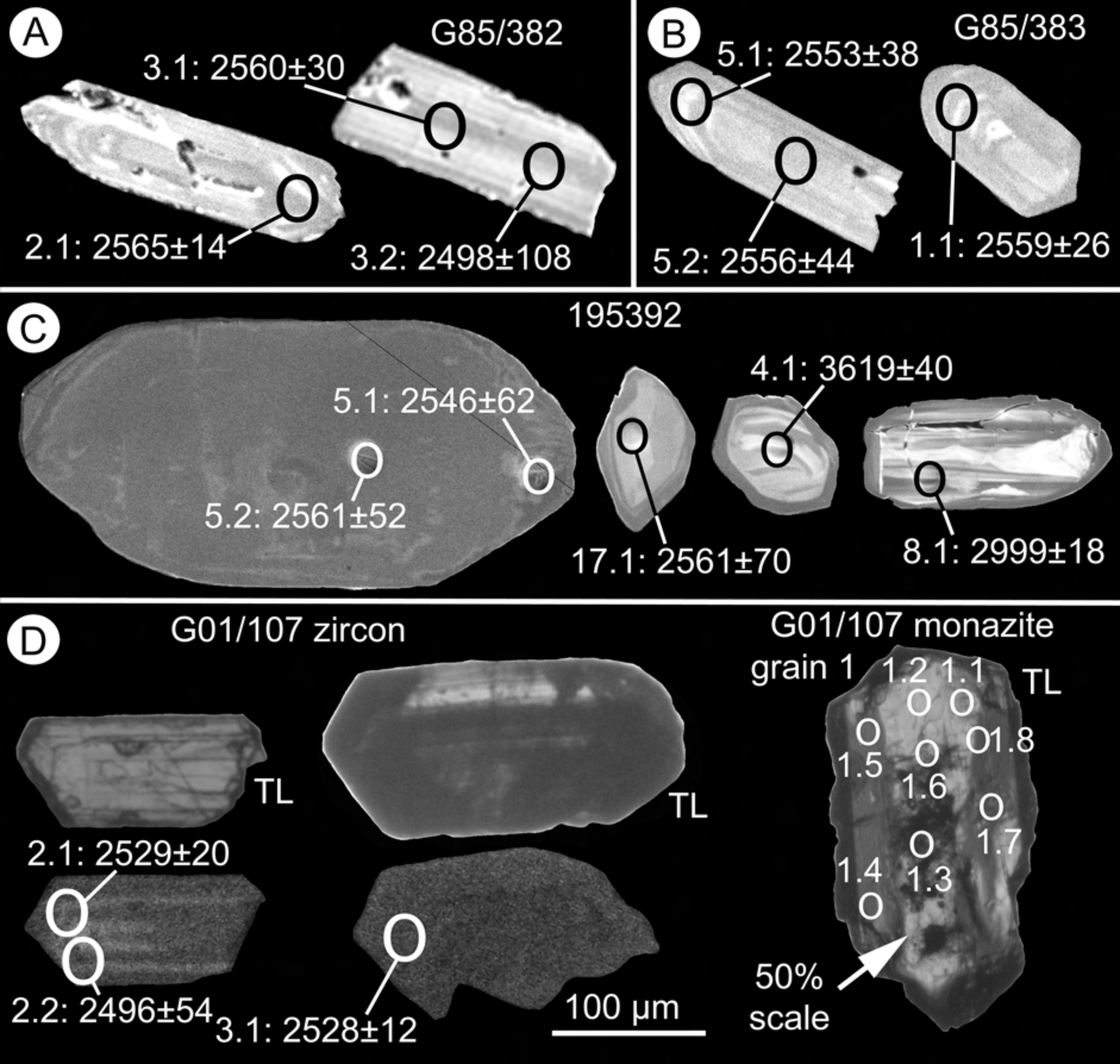
A
G85/382
3.1: 2560±30
2.1: 2565±14
3.2: 2498±108
B
G85/383
5.1: 2553±38
5.2: 2556±44
1.1: 2559±26
C
195392
5.1: 2546±62
5.2: 2561±52
4.1: 3619±40
17.1: 2561±70
8.1: 2999±18
D
G01/107 zircon
TL
TL
2.1: 2529±20
2.2: 2496±54
3.1: 2528±12
100 µm
G01/107 monazite
grain 1
1.2
1.1
TL
1.8
1.5
1.6
1.7
1.4
1.3
50%
scale

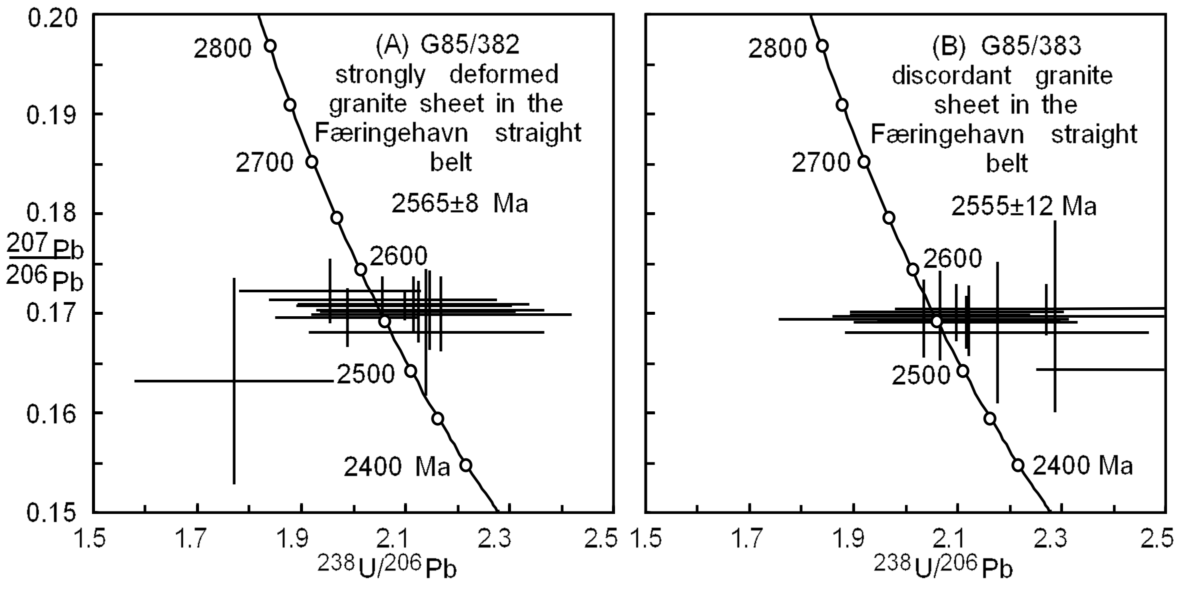

(A) G85/382
strongly deformed granite sheet in the Færingehavn straight belt
2565±8 Ma
2800
2700
2600
2500
2400 Ma
0.20
0.19
0.18
0.17
0.16
0.15
$^{207}Pb/^{206}Pb$
1.5
1.7
1.9
2.1
2.3
2.5
$^{238}U/^{206}Pb$
(B) G85/383
discordant granite sheet in the Færingehavn straight belt
2555±12 Ma
2800
2700
2600
2500
2400 Ma
1.5
1.7
1.9
2.1
2.3
2.5
$^{238}U/^{206}Pb$

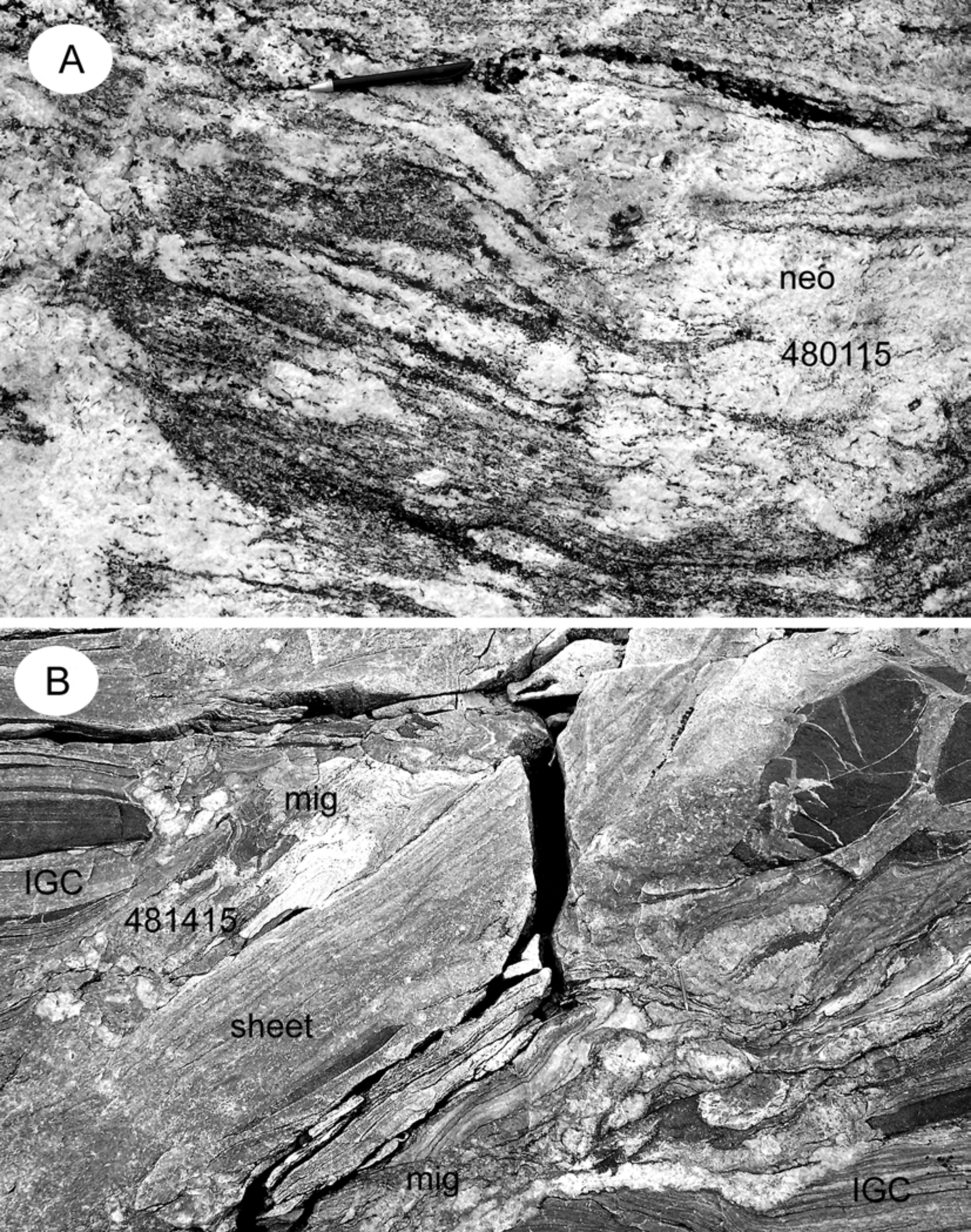
A
neo
480115
B
mig
IGC
481415
sheet
mig
IGC

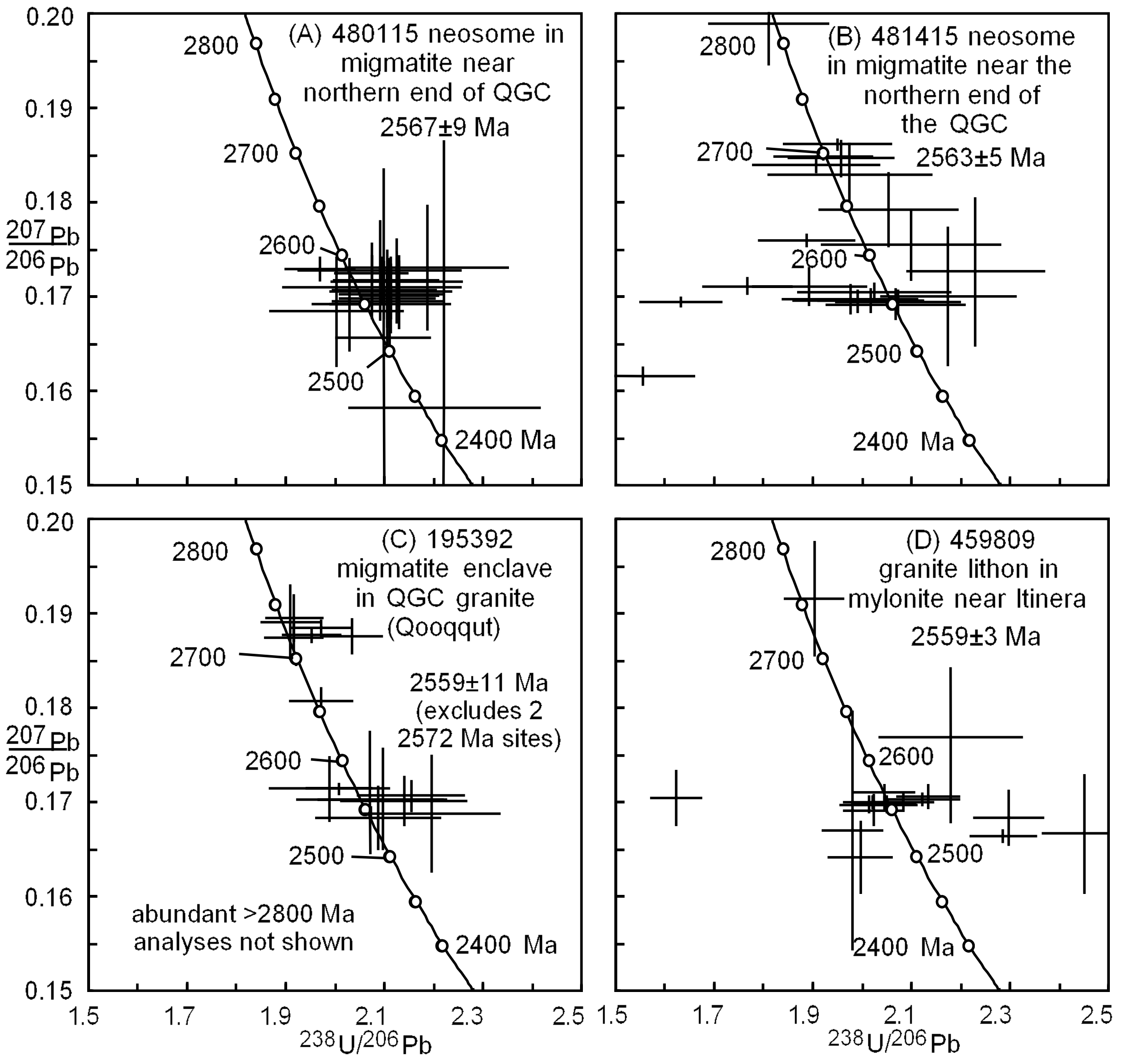

(A) 480115 neosome in migmatite near northern end of QGC
2567±9 Ma
(B) 481415 neosome in migmatite near the northern end of the QGC
2563±5 Ma
(C) 195392 migmatite enclave in QGC granite (Qooqqut)
2559±11 Ma (excludes 2 2572 Ma sites)
abundant >2800 Ma analyses not shown
(D) 459809 granite lithon in mylonite near Itinera
2559±3 Ma
2800
2700
2600
2500
2400 Ma
207Pb/206Pb
238U/206Pb
0.15
0.16
0.17
0.18
0.19
0.20
1.5
1.7
1.9
2.1
2.3
2.5

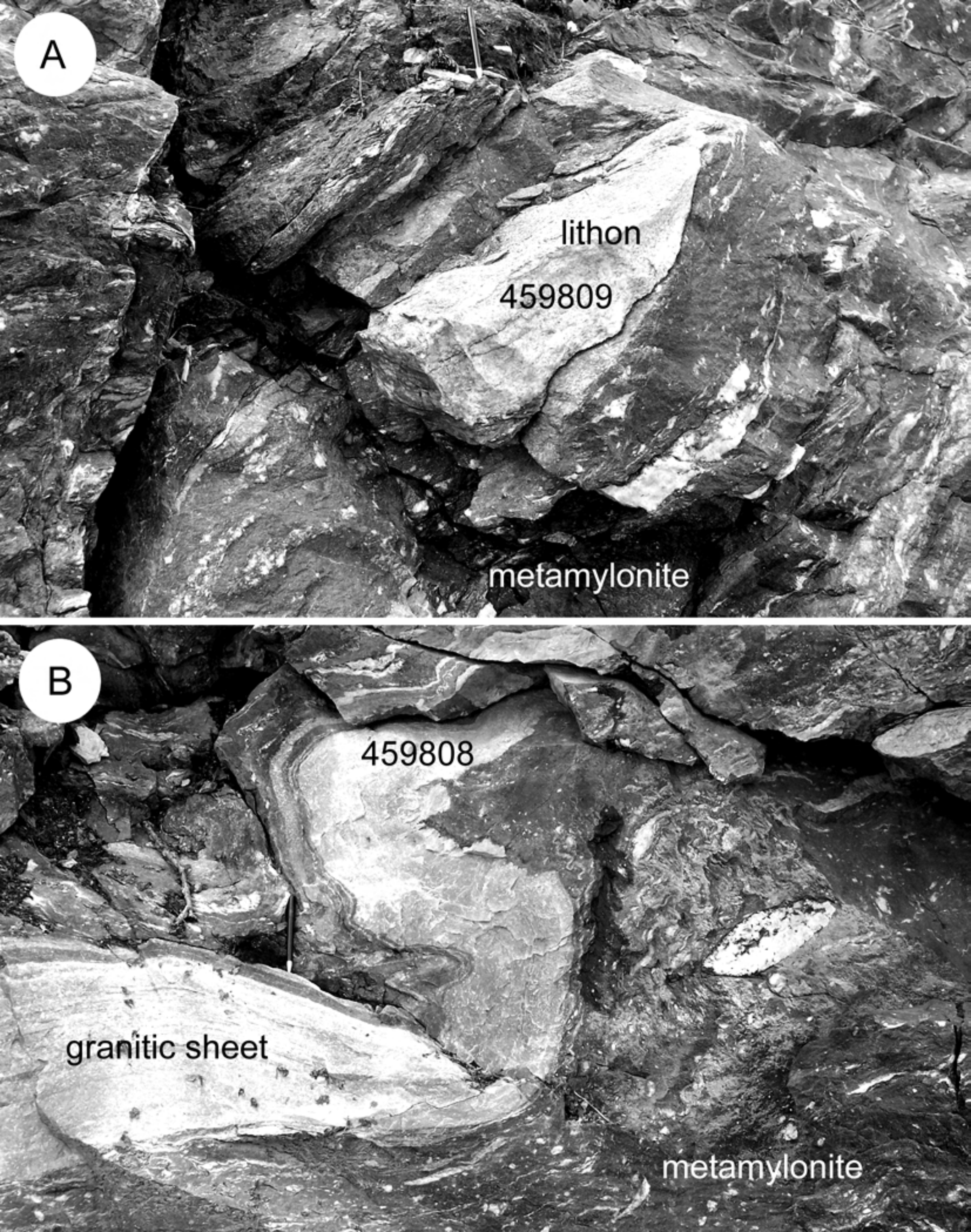
A
lithon
459809
metamylonite
B
459808
granitic sheet
metamylonite

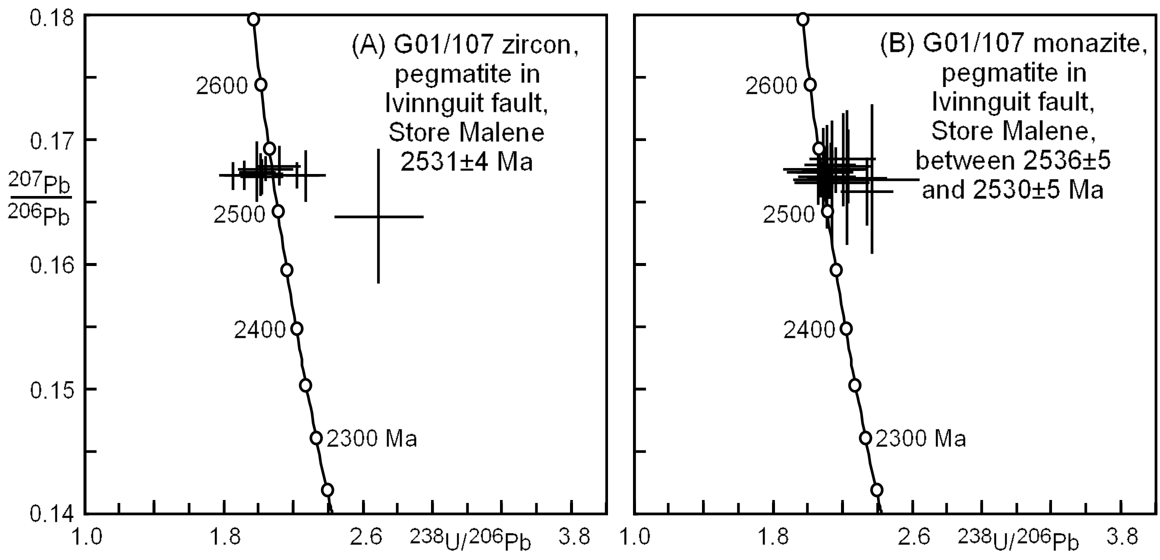

(A) G01/107 zircon, pegmatite in Ivinnguit fault, Store Malene 2531±4 Ma
(B) G01/107 monazite, pegmatite in Ivinnguit fault, Store Malene, between 2536±5 and 2530±5 Ma
$^{207}Pb/^{206}Pb$
$^{238}U/^{206}Pb$
0.18
0.17
0.16
0.15
0.14
1.0
1.8
2.6
3.8
2600
2500
2400
2300 Ma

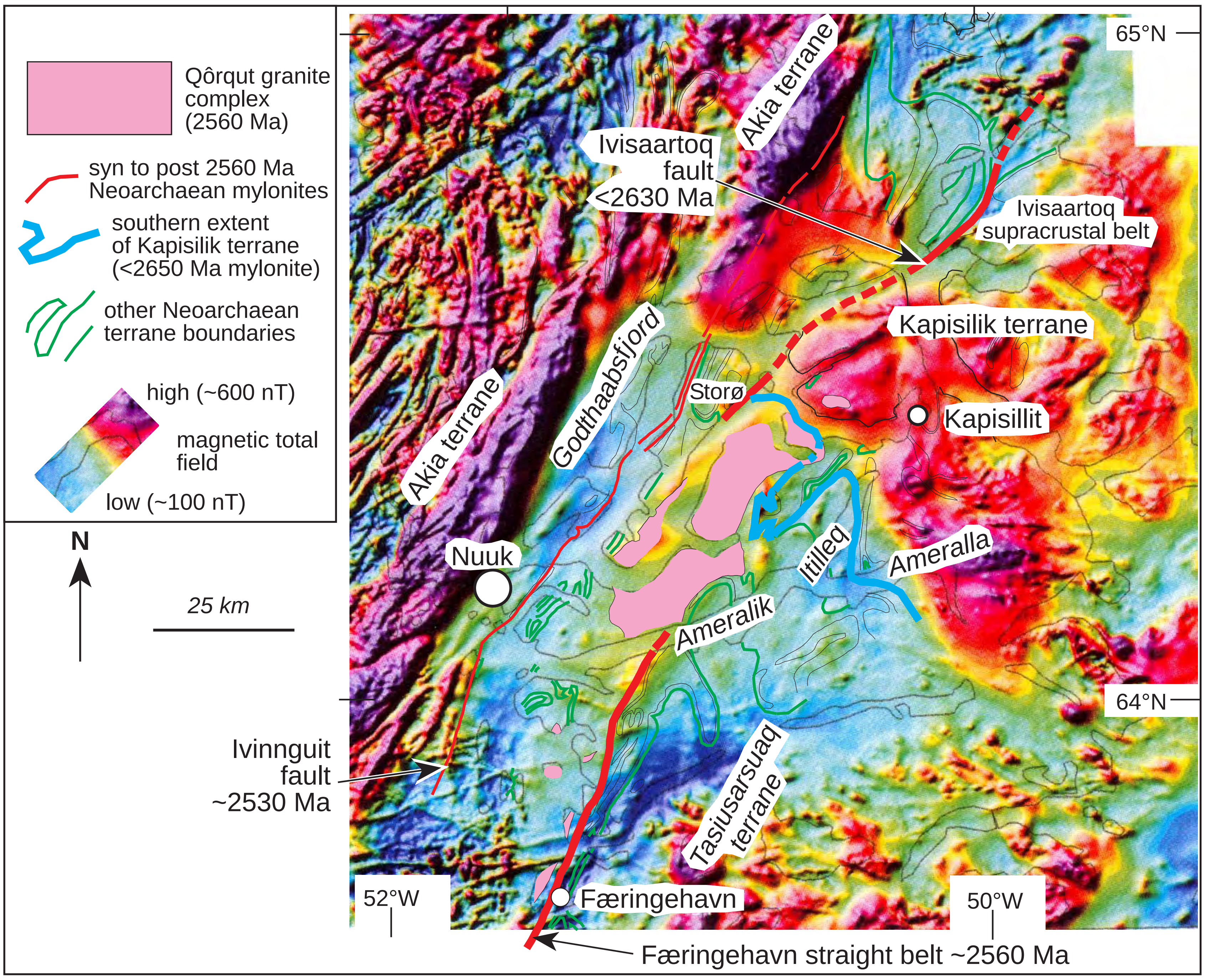

Qôrqut granite complex (2560 Ma)
syn to post 2560 Ma Neoarchaean mylonites
southern extent of Kapisilik terrane (<2650 Ma mylonite)
other Neoarchaean terrane boundaries
high (~600 nT)
magnetic total field
low (~100 nT)
N
25 km
65°N
64°N
52°W
50°W
Akia terrane
Ivisaartoq fault <2630 Ma
Ivisaartoq supracrustal belt
Kapisilik terrane
Godthaabsfjord
Storø
Kapisillit
Akia terrane
Nuuk
Itilleq
Ameralla
Ameralik
Ivinnguit fault ~2530 Ma
Tasiusarsuaq terrane
Færingehavn
Færingehavn straight belt ~2560 Ma

Table 1. SHRIMP U-Pb zircon and monazite analyses

spot	site type	U ppm	Th ppm	Th/U	comm. 206Pb%	238U / 206Pb ratio	207Pb / 206Pb ratio	207 / 206 age	conc. %
16.1	e,osc,p	578	832	1.44	1.05	2.100 ± 0.052	0.1708 ± 0.0015	2565 ± 15	98
17.1	e,osc,p	692	1187	1.72	3.19	2.113 ± 0.060	0.1693 ± 0.0024	2550 ± 24	98
18.1	e,osc,p	445	439	0.99	0.09	2.003 ± 0.067	0.1685 ± 0.0029	2543 ± 29	103
19.1	m,osc,p	687	832	1.21	0.86	2.030 ± 0.037	0.1692 ± 0.0024	2550 ± 24	101
20.1	e,osc,p	672	419	0.62	3.07	2.606 ± 0.092	0.1714 ± 0.0043	2571 ± 43	81
21.1	osc,p	691	707	1.02	1.95	2.075 ± 0.037	0.1725 ± 0.0016	2582 ± 15	98

481415 weakly deformed neosome in migmatites, at northern end of the QGC: 2563±5 Ma

spot	site type	U ppm	Th ppm	Th/U	comm. 206Pb%	238U / 206Pb ratio	207Pb / 206Pb ratio	207 / 206 age	conc. %
1.1	e,osc,eq	108	60	0.56	0.02	2.098 ± 0.090	0.1755 ± 0.0019	2611 ± 18	96
2.1	e,osc/h,p	2971	208	0.07	0.29	1.990 ± 0.065	0.1695 ± 0.0006	2553 ± 6	103
3.1	m/c,osc,p	294	125	0.42	0.23	1.973 ± 0.082	0.1829 ± 0.0017	2680 ± 15	99
4.1	e,osc/h,p	1497	95	0.06	<0.01	2.067 ± 0.070	0.1692 ± 0.0008	2550 ± 8	100
5.1	e,osc,p	7720	348	0.05	0.08	1.630 ± 0.041	0.1694 ± 0.0002	2552 ± 2	121
6.1	e,osc,p	1718	109	0.06	<0.01	1.919 ± 0.049	0.1850 ± 0.0002	2698 ± 2	100
7.1	e.osc,p	163	17	0.10	0.03	1.280 ± 0.048	0.3350 ± 0.0024	3640 ± 11	102
8.1	e.osc,p	7540	2498	0.33	0.02	1.555 ± 0.051	0.1616 ± 0.0004	2472 ± 5	130
9.1	m,osc,p,fr	110	95	0.86	0.02	1.274 ± 0.047	0.3387 ± 0.0019	3657 ± 8	102
10.1	e,osc,p	2778	183	0.07	<0.01	1.905 ± 0.064	0.1841 ± 0.0004	2690 ± 4	101
11.1	e,osc,p	852	315	0.37	0.15	2.023 ± 0.077	0.1705 ± 0.0004	2562 ± 4	101
12.1	m,osc,p	126	112	0.89	0.07	1.892 ± 0.057	0.1711 ± 0.0010	2568 ± 10	107
13.1	e,osc,p	1382	899	0.65	0.01	2.015 ± 0.052	0.1696 ± 0.0006	2554 ± 6	102
14.1	e,osc,p	3267	112	0.03	<0.01	1.885 ± 0.048	0.1760 ± 0.0003	2615 ± 3	105
15.1	e,h,p	888	71	0.08	0.13	1.974 ± 0.068	0.1698 ± 0.0007	2555 ± 7	103
16.1	e,hd,anh	1824	183	0.10	<0.01	2.070 ± 0.062	0.1694 ± 0.0006	2552 ± 6	100
17.1	e,osc,p	2638	785	0.30	0.03	1.766 ± 0.045	0.1712 ± 0.0004	2569 ± 4	113
18.1	m,osc,p	604	196	0.32	0.07	1.359 ± 0.060	0.3270 ± 0.0043	3603 ± 20	99
19.1	composite,p	849	31	0.04	0.79	1.517 ± 0.041	0.2756 ± 0.0012	3338 ± 7	98
20.1	e,osc,p	200	58	0.29	0.15	1.956 ± 0.053	0.1847 ± 0.0009	2696 ± 8	99
21.1	e,osc,eq	211	126	0.59	1.45	2.173 ± 0.068	0.1701 ± 0.0037	2558 ± 36	95
22.1	e,osc/rex,p	435	85	0.20	0.15	1.381 ± 0.037	0.3186 ± 0.0034	3563 ± 16	99
23.1	e,osc,eq,fr	287	94	0.33	1.53	2.052 ± 0.069	0.1793 ± 0.0019	2646 ± 18	97
24.1	composite,p	792	51	0.06	0.06	1.431 ± 0.039	0.2954 ± 0.0012	3446 ± 6	99
25.1	e,osc,p	403	142	0.35	0.02	1.332 ± 0.035	0.3391 ± 0.0010	3659 ± 5	99
26.1	m,osc,p	502	273	0.54	12.59	2.228 ± 0.069	0.1727 ± 0.0039	2584 ± 38	93
27.1	e,osc,p	159	158	1.00	0.03	1.809 ± 0.060	0.1991 ± 0.0022	2818 ± 18	101
28.1	m,h,p	1565	27	0.02	0.01	1.277 ± 0.035	0.3364 ± 0.0010	3646 ± 4	102
29.1	e,osc,p	1581	640	0.40	0.01	1.948 ± 0.054	0.1862 ± 0.0003	2709 ± 2	99

195392 migmatite with QGC component, north side of Qooqqut: 2559±11 Ma

spot	site type	U ppm	Th ppm	Th/U	comm. 206Pb%	238U / 206Pb ratio	207Pb / 206Pb ratio	207 / 206 age	conc. %
1.1	c,osc,p	248	119	0.48	<0.01	1.388 ± 0.041	0.3459 ± 0.0016	3689 ± 7	95
2.2	e,h,p	796	35	0.04	0.04	2.155 ± 0.054	0.1707 ± 0.0008	2564 ± 8	96
3.1	m,osc,p	180	67	0.37	0.19	2.087 ± 0.062	0.1684 ± 0.0017	2541 ± 16	99
4.1	c,osc,p	42	39	0.93	0.08	1.348 ± 0.046	0.3305 ± 0.0042	3619 ± 20	99
5.1	e,h,p	61	32	0.51	0.07	2.196 ± 0.069	0.1688 ± 0.0031	2546 ± 31	95
5.2	m,h,p	98	70	0.72	0.28	2.097 ± 0.064	0.1704 ± 0.0027	2561 ± 26	98
6.1	c,osc,p	53	53	1.00	<0.01	1.591 ± 0.051	0.3046 ± 0.0034	3494 ± 17	91
7.1	c,osc,p	43	32	0.75	0.12	1.811 ± 0.060	0.2355 ± 0.0051	3090 ± 35	92
8.1	c,osc,p	396	31	0.08	0.29	1.866 ± 0.055	0.2226 ± 0.0012	2999 ± 9	92
9.1	c,osc,p	124	51	0.41	1.15	1.946 ± 0.059	0.2202 ± 0.0028	2982 ± 21	91
10.1	c,osc,p	134	109	0.81	<0.01	1.409 ± 0.043	0.3274 ± 0.0020	3605 ± 10	96
11.1	c,osc,p	1291	296	0.23	0.01	1.798 ± 0.052	0.2325 ± 0.0006	3069 ± 4	93
12.1	e,h,p	104	54	0.53	0.47	1.989 ± 0.060	0.1714 ± 0.0017	2572 ± 17	102
13.1	c,osc,p	103	40	0.38	0.42	1.797 ± 0.059	0.2253 ± 0.0021	3019 ± 15	95
15.1	c,osc,p	64	25	0.39	0.58	1.727 ± 0.055	0.2548 ± 0.0048	3215 ± 30	92
15.2	c,osc,p	94	37	0.39	0.33	1.447 ± 0.043	0.3254 ± 0.0017	3596 ± 8	94
16.1	c,osc,p	183	46	0.25	0.14	1.321 ± 0.041	0.3552 ± 0.0042	3729 ± 18	97
17.1	m,osc/h,p	42	43	1.03	1.34	2.071 ± 0.074	0.1704 ± 0.0036	2561 ± 35	99
18.1	e,h,p	151	61	0.41	0.39	2.140 ± 0.063	0.1702 ± 0.0013	2559 ± 13	97
B-1.1	c,osc,p	239	116	0.50	0.05	1.361 ± 0.023	0.3401 ± 0.0009	3663 ± 4	97
B-1.2	m,osc,p	1316	494	0.39	<0.01	1.262 ± 0.019	0.3447 ± 0.0003	3684 ± 1	102
B-2.2	c,osc,anh	824	72	0.09	0.11	1.953 ± 0.029	0.1878 ± 0.0003	2723 ± 3	98
B-3.1	e,osc,p	214	27	0.13	0.13	1.972 ± 0.031	0.1808 ± 0.0006	2660 ± 6	99
B-4.1	m,osc,p	166	260	1.62	0.27	1.410 ± 0.033	0.3366 ± 0.0009	3647 ± 4	94
B-5.2	e,h,anh	1258	56	0.05	0.01	2.008 ± 0.033	0.1715 ± 0.0002	2572 ± 2	101
B-6.1	m,osc,p	309	20	0.07	0.50	2.034 ± 0.031	0.1877 ± 0.0009	2722 ± 8	94
B-6.2	c,osc,p	1026	37	0.04	0.15	1.459 ± 0.021	0.3271 ± 0.0008	3603 ± 4	93
B-8.1	m,osc,p	357	24	0.07	0.86	1.918 ± 0.029	0.1896 ± 0.0012	2739 ± 10	99
B-8.2	c,osc,p	1244	86	0.07	<0.01	1.321 ± 0.021	0.3324 ± 0.0006	3628 ± 3	100
B-8.3	e,osc,p	250	18	0.07	1.36	1.910 ± 0.029	0.1891 ± 0.0019	2735 ± 17	99
B-8.4	c,osc,p	904	90	0.10	0.06	1.358 ± 0.020	0.3306 ± 0.0003	3620 ± 2	98
B-9.1	m,osc,p	205	20	0.10	0.25	1.918 ± 0.029	0.1875 ± 0.0007	2721 ± 6	99
B-9.2	c,osc,p	570	53	0.10	0.04	1.973 ± 0.030	0.1886 ± 0.0003	2730 ± 3	97
B-10.1	m,h,anh	1462	50	0.04	0.03	1.305 ± 0.021	0.3351 ± 0.0003	3640 ± 1	101
B-11.1	c,h,anh	1476	56	0.04	<0.01	1.365 ± 0.020	0.3254 ± 0.0009	3595 ± 4	99
B-12.1	m,osc,p	254	28	0.11	0.10	1.495 ± 0.026	0.3168 ± 0.0007	3555 ± 3	92

459809 granite lithon in mylonite, Kapisillit fjord: 2559±3 Ma

spot	site type	U ppm	Th ppm	Th/U	comm. 206Pb%	238U / 206Pb ratio	207Pb / 206Pb ratio	207 / 206 age	conc. %
1.1	e,hd,p	1808	1850	1.06	0.82	2.298 ± 0.035	0.1684 ± 0.0014	2541 ± 14	109

Table 1. SHRIMP U-Pb zircon and monazite analyses

spot	site type	U ppm	Th ppm	Th/U	comm. 206Pb%	238U / 206/Pb ratio	207Pb / 206Pb ratio	207 / 206 age	conc. %
2.1	m,hd,p	1239	1578	1.32	2.47	2.452 ± 0.042	0.1667 ± 0.0031	2524 ± 31	114
3.1	m,hd,anh	1496	1848	1.28	0.01	2.122 ± 0.037	0.1703 ± 0.0003	2560 ± 3	103
4.1	m,osc,p	642	675	1.09	3.53	2.180 ± 0.072	0.1770 ± 0.0045	2624 ± 42	108
4.2	e,hd,p	1126	1155	1.06	0.13	2.085 ± 0.030	0.1701 ± 0.0004	2558 ± 4	101
5.1	m,hd,p	3363	3874	1.19	0.13	2.287 ± 0.033	0.1665 ± 0.0003	2522 ± 3	108
6.1	m,hd,anh	1332	1840	1.43	0.00	2.135 ± 0.031	0.1706 ± 0.0006	2564 ± 6	104
7.1	m,hd,p	4744	455	0.10	0.68	1.997 ± 0.032	0.1642 ± 0.0019	2499 ± 20	96
8.1	m,hd,p	605	440	0.75	1.77	1.903 ± 0.029	0.1916 ± 0.0030	2756 ± 26	101
8.2	m,hd,p	1079	1087	1.04	0.07	2.046 ± 0.030	0.1711 ± 0.0004	2568 ± 4	100
9.1	m,hd,p	3333	2378	0.74	0.02	2.024 ± 0.030	0.1692 ± 0.0008	2550 ± 8	99
10.1	e,hd,p	1667	2218	1.38	4.96	1.982 ± 0.030	0.1671 ± 0.0063	2529 ± 63	96
11.1	m,hd,p	1535	2350	1.58	0.01	2.023 ± 0.029	0.1700 ± 0.0003	2557 ± 3	99
12.1	c,hd,anh,fr	940	754	0.83	0.03	2.045 ± 0.032	0.1699 ± 0.0004	2556 ± 4	100
13.1	c,hd,anh,fr	873	814	0.96	0.05	2.051 ± 0.030	0.1698 ± 0.0004	2556 ± 4	100
14.1	e,hd,p	3992	1175	0.30	1.14	1.624 ± 0.025	0.1705 ± 0.0014	2562 ± 14	83
15.1	m,hd,p	1859	93	0.05	0.01	2.015 ± 0.029	0.1698 ± 0.0004	2556 ± 4	98

459808 folded granite sheet in mylonite, Kapisillit fjord: 2446±88 Ma concordia intercept

spot	site type	U ppm	Th ppm	Th/U	comm. 206Pb%	238U / 206/Pb ratio	207Pb / 206Pb ratio	207 / 206 age	conc. %
1.1	e,hd,p	8569	36091	4.35	3.56	30.683 ± 0.454	0.1384 ± 0.0046	2207 ± 58	9
2.1	m,hd,p	4693	23496	5.17	0.31	20.550 ± 0.316	0.1530 ± 0.0012	2380 ± 13	13
3.1	m,hd,p	1741	5874	3.49	1.83	6.257 ± 0.208	0.1622 ± 0.0035	2479 ± 36	39
4.1	m,hd,p	7586	14210	1.94	2.13	10.095 ± 0.159	0.1559 ± 0.0027	2412 ± 29	25
5.1	m,hd,p	2000	12698	6.56	2.27	13.392 ± 0.199	0.1575 ± 0.0034	2429 ± 37	19
6.1	m,hd,p	7409	12218	1.70	0.61	13.626 ± 0.202	0.1526 ± 0.0009	2375 ± 10	19
7.1	m,hd,p	8622	20795	2.49	1.63	15.282 ± 0.221	0.1527 ± 0.0020	2376 ± 23	17
8.1	c,osc,p	477	809	1.75	5.34	2.166 ± 0.035	0.2894 ± 0.0081	3414 ± 44	72

G01/107 deformed granite sheet cutting Ivinnguit fault mylonite near Nuuk:
zircons 2531±4 Ma

spot	site type	U ppm	Th ppm	Th/U	comm. 206Pb%	238U / 206/Pb ratio	207Pb / 206Pb ratio	207 / 206 age	conc. %
1.1	e,osc,p	2972	238	0.08	0.01	2.043 ± 0.075	0.1677 ± 0.0005	2534 ± 5	101
2.1	e,osc,p	2213	272	0.12	0.02	2.273 ± 0.055	0.1671 ± 0.0010	2529 ± 10	93
2.2	e,osc,p	1883	244	0.13	2.54	2.690 ± 0.125	0.1638 ± 0.0027	2496 ± 27	82
3.1	e,osc,p	2069	159	0.08	<0.01	2.017 ± 0.059	0.1670 ± 0.0006	2528 ± 6	103
4.1	e,hd,p	3617	430	0.12	<0.01	1.856 ± 0.037	0.1671 ± 0.0005	2529 ± 5	110
5.1	e,hd,p	3233	433	0.13	0.01	2.120 ± 0.058	0.1679 ± 0.0007	2536 ± 7	98
6.1	e,hd,p	3113	455	0.15	0.01	1.918 ± 0.053	0.1672 ± 0.0005	2529 ± 5	107
7.1	e,hd,p	2579	350	0.14	<0.01	1.993 ± 0.050	0.1674 ± 0.0012	2532 ± 12	104
8.1	e,hd,p	2553	349	0.14	0.01	2.013 ± 0.059	0.1672 ± 0.0008	2530 ± 8	103
9.1	e,hd,p	2356	325	0.14	0.11	5.358 ± 0.172	0.1426 ± 0.0008	2259 ± 10	49
10.1	e,osc,p	1962	108	0.05	0.01	2.221 ± 0.062	0.1671 ± 0.0005	2529 ± 5	95

G01/107 deformed granite sheet cutting Ivinnguit fault mylonite near Nuuk:
monazites 2536±5 Ma (uncorrected), 2530±5 Ma (overcorrected)
(corrected data shown)

spot	site type	U ppm	Th ppm	Th/U	comm. 206Pb%	238U / 206/Pb ratio	207Pb / 206Pb ratio	207 / 206 age	conc. %
1.1		4204	148380	35.3	0.06	2.090 ± 0.113	0.1676 ± 0.0016	2534 ± 16	100
1.2		4215	149747	35.5	0.06	2.058 ± 0.085	0.1673 ± 0.0012	2531 ± 12	101
1.3		3442	122886	35.7	0.18	2.225 ± 0.111	0.1670 ± 0.0026	2527 ± 27	95
1.4		2485	68031	27.4	0.01	2.342 ± 0.072	0.1659 ± 0.0013	2516 ± 13	91
1.5		2145	80493	37.5	0.00	2.233 ± 0.064	0.1679 ± 0.0014	2537 ± 14	94
1.6		3238	115203	35.6	0.05	2.124 ± 0.096	0.1665 ± 0.0006	2523 ± 6	99
1.7		2613	98429	37.7	0.06	2.127 ± 0.071	0.1680 ± 0.0009	2537 ± 9	98
1.8		2586	98443	38.1	<0.01	2.099 ± 0.076	0.1674 ± 0.0008	2531 ± 8	99
2.1		2324	121637	52.3	0.05	2.074 ± 0.076	0.1668 ± 0.0006	2526 ± 6	100
2.2		1619	57171	35.3	0.03	2.200 ± 0.093	0.1684 ± 0.0018	2542 ± 18	95
2.3		2819	133241	47.3	0.03	2.140 ± 0.075	0.1677 ± 0.0007	2534 ± 7	98
3.1		1113	86472	77.7	0.13	2.369 ± 0.134	0.1668 ± 0.0029	2526 ± 30	90
3.2		1178	90267	76.6	0.05	2.162 ± 0.081	0.1676 ± 0.0009	2534 ± 9	97
3.3		1454	103635	71.3	0.08	2.111 ± 0.079	0.1670 ± 0.0020	2528 ± 21	99
4.1		1625	96383	59.3	0.26	2.106 ± 0.067	0.1676 ± 0.0009	2534 ± 9	99
4.2		1161	80459	69.3	0.08	2.140 ± 0.104	0.1666 ± 0.0024	2524 ± 25	98

414415 deformed granite sheet in shear zone, northern edge of craton: 2492±11 Ma

spot	site type	U ppm	Th ppm	Th/U	comm. 206Pb%	238U / 206/Pb ratio	207Pb / 206Pb ratio	207 / 206 age	conc. %
1.1	osc,p	151	217	1.44	0.10	2.165 ± 0.109	0.1622 ± 0.0050	2479 ± 53	99
2.1	osc,p	45	32	0.72	0.84	2.053 ± 0.068	0.1622 ± 0.0035	2479 ± 37	103
3.1	osc,p	75	56	0.75	0.37	2.073 ± 0.079	0.1637 ± 0.0017	2495 ± 18	102
4.1	osc,p	52	55	1.05	0.87	2.093 ± 0.067	0.1630 ± 0.0031	2487 ± 32	101
6.1	osc,p	77	38	0.49	0.09	2.108 ± 0.054	0.1661 ± 0.0021	2519 ± 21	99
7.1	osc,p	114	89	0.78	0.10	2.161 ± 0.053	0.1636 ± 0.0012	2493 ± 13	98
8.1	osc,p	120	89	0.74	0.09	2.188 ± 0.095	0.1650 ± 0.0012	2508 ± 12	97
9.1	osc,p	54	41	0.76	1.11	2.104 ± 0.060	0.1577 ± 0.0028	2432 ± 30	103
10.1	osc,p	172	51	0.30	0.22	2.188 ± 0.059	0.1611 ± 0.0016	2467 ± 17	98
11.1	osc,p	34	31	0.89	1.19	2.096 ± 0.069	0.1587 ± 0.0039	2442 ± 42	103
12.1	osc,p	65	33	0.50	0.46	2.044 ± 0.065	0.1637 ± 0.0019	2494 ± 19	103
13.1	osc,p	71	90	1.26	0.11	2.126 ± 0.069	0.1617 ± 0.0016	2473 ± 17	101

VM95/03 deformed granite sheet, southern edge of craton: 2540±11 Ma

spot	site type	U ppm	Th ppm	Th/U	comm. 206Pb%	238U / 206/Pb ratio	207Pb / 206Pb ratio	207 / 206 age	conc. %
1.1	osc,p	182	124	0.68	0.17	2.248 ± 0.058	0.1685 ± 0.0007	2543 ± 7	93

Table 1. SHRIMP U-Pb zircon and monazite analyses

spot	site type	U ppm	Th ppm	Th/U	comm. 206Pb%	238U / 206/Pb ratio	207Pb / 206Pb ratio	207 / 206 age	conc. %
2.1	osc,p	555	237	0.43	0.05	2.902 ± 0.117	0.1662 ± 0.0016	2519 ± 16	76
3.1	fr	269	354	1.31	0.03	1.852 ± 0.041	0.2025 ± 0.0008	2846 ± 6	98
4.1	fr	680	102	0.15	0.10	2.063 ± 0.271	0.1874 ± 0.0042	2720 ± 37	94
5.1	osc,p	57	49	0.85	0.05	2.215 ± 0.066	0.1683 ± 0.0018	2541 ± 18	95

first column: grain number followed by analysis number. Those used in age determinations are shown bold.
grain morphology: p=prism, fr=fragment, eq=equant, bipyramidal or oval, anh=anhedral
CL imagery: rex=recrystallised, osc=oscillatory zoning, sz=sector zoning, h=homogeneous, hd=dark in CL images
corrected with 3600 Ma model Pb of Cumming and Richards, 1975; all errors quoted at 1 sigma